



Measurements of azimuthal anisotropies of jet production in Pb+Pb collisions at $\sqrt{s_{NN}} = 5.02$ TeV with the ATLAS detector

The ATLAS Collaboration

The azimuthal variation of jet yields in heavy-ion collisions provides information about the path-length dependence of the energy loss experienced by partons passing through the hot, dense nuclear matter known as the quark–gluon plasma. This paper presents the azimuthal anisotropy coefficients v_2 , v_3 , and v_4 measured for jets in Pb+Pb collisions at $\sqrt{s_{NN}} = 5.02$ TeV using the ATLAS detector at the LHC. The measurement uses data collected in 2015 and 2018, corresponding to an integrated luminosity of 2.2 nb^{-1} . The v_n values are measured as a function of the transverse momentum of the jets between 71 GeV and 398 GeV and the event centrality. A nonzero value of v_2 is observed in all but the most central collisions. The value of v_2 is largest for jets with lower transverse momentum, with values up to 0.05 in mid-central collisions. A smaller, nonzero value of v_3 of approximately 0.01 is measured with no significant dependence on jet p_T or centrality, suggesting that fluctuations in the initial state play a small but distinct role in jet energy loss. No significant deviation of v_4 from zero is observed in the measured kinematic region.

Contents

1	Introduction	3
2	ATLAS detector and trigger	4
3	Data and event selection	5
4	Analysis procedure	6
5	Systematic uncertainties	8
6	Results	13
7	Conclusion	20

1 Introduction

The primary physics aim of the heavy-ion program at the Large Hadron Collider (LHC) is to produce and study the quark–gluon plasma (QGP), the high-temperature state of quantum-chromodynamic matter in which quarks and gluons are no longer confined within protons and neutrons (for a recent review, see Ref. [1]). Measurements of jets produced in the early stages of heavy-ion collisions provide information about the short-distance-scale interactions of high-energy partons with the QGP. The overall rate of jets in central Pb+Pb collisions at a given transverse momentum p_T is found to be about a factor of two lower than expectations based on pp collisions, up to a p_T of approximately 1 TeV [2, 3]. This suppression can be explained by the downward slope of the jet p_T spectrum and the reduction in parton p_T due to energy loss while traversing the QGP. The energy loss from partons is expected to depend on the length of the QGP region that the parton traverses. The geometry of the overlapping nuclei in mid-central collisions leads to shorter average path lengths if the jet is oriented along the direction of the collision impact parameter¹ than if the jet is oriented in the perpendicular direction. This should lead to a dependence of the jet yield on the azimuthal angle [4–6].

One key observable in understanding the path-length dependence of energy loss is the azimuthal anisotropy of jets. The azimuthal distribution of jets is described via a Fourier expansion:

$$\frac{dN_{\text{jet}}}{d\phi} \propto 1 + 2 \sum_{n=1}^{\infty} v_n \cos(n(\phi - \Psi_n)),$$

where the v_n and Ψ_n are the magnitude and orientation of the n^{th} -order anisotropy, and ϕ is the azimuthal angle of jets. The Ψ_n , or event-plane angles, are oriented such that a jet produced in-plane, or along the direction of the event-plane angle, will traverse on average less QGP than a jet produced out-of-plane, or perpendicular to the event-plane angle. Similar Fourier expansions are often used to describe the azimuthal variation of the yield of soft particles, which is typically associated with hydrodynamic flow (see Ref. [7]). It is important to note that at high p_T , hydrodynamic flow is not expected to be the source of azimuthal variation. Measurements of the v_n for high- p_T particles have been performed at the Relativistic Heavy Ion Collider (RHIC) [8, 9]. The first measurement of the v_2 for fully reconstructed jets was reported in Ref. [10] for Pb+Pb collisions at $\sqrt{s_{\text{NN}}} = 2.76$ TeV. The measured v_2 values were found to be positive for jets with transverse momentum 45–160 GeV. The v_2 values were found to be smaller in the most central and most peripheral collisions. This is expected because the second-order eccentricity of the initial state is small in the most central collisions, while in the most peripheral collisions there is little energy loss in any direction. A measurement by ALICE using jets reconstructed from charged particles obtained similar results [11]. Related measurements by CMS and ATLAS have been performed with charged particles at high p_T in 5.02 TeV Pb+Pb collisions [12, 13]. Reference [12] reported positive v_2 values for charged particles with p_T up to 60–80 GeV. Until now, there have been no measurements of jet v_2 in $\sqrt{s_{\text{NN}}} = 5.02$ TeV Pb+Pb collisions and no measurements of the higher-order anisotropies, such as v_3 and v_4 , of jets in any collision system. Such measurements could provide new information about how the energy loss depends on path length and the initial collision geometry.

Recent calculations have shown that realistic modeling of both the jet energy loss and the soft fluctuations are necessary to reproduce the experimental measurements of high- p_T particles [14]. Therefore, it is of interest to study observables that are sensitive to both path-length dependence of the energy loss and

¹ The impact parameter is the distance between the centers of the colliding nuclei in the plane transverse to the collision axis.

fluctuations of the initial collision geometry, such as the dependence of the jet yield on higher-order eccentricities of the initial state [15].

The results presented here extend the measurement of jet azimuthal anisotropy to higher jet p_T than in previous measurements and to a collision energy of $\sqrt{s_{\text{NN}}} = 5.02$ TeV. Additionally, higher-order harmonics, v_3 and v_4 , are measured. The measurement utilizes 2.2 nb^{-1} of Pb+Pb data collected at $\sqrt{s_{\text{NN}}} = 5.02$ TeV in 2015 and 2018. Jets are reconstructed using the anti- k_t [16] algorithm with $R = 0.2$. Compared to larger-radius jets, these small-radius jets provide improved angular resolution for the estimation of the jet axis; this improvement is due to the smaller underlying event within the jet cone, which helps in measuring the angular anisotropies. The jets used in this analysis are restricted to rapidities $|y| < 1.2$.² The observed event-plane angles, Ψ_n^{obs} , are reconstructed using the transverse energy measured over $4.0 < |\eta| < 4.9$ as described in Section 4 and the v_n^{obs} values are extracted by fitting independently for each order, n :

$$\frac{dN_{\text{jet}}(p_T, \Delta\phi_n)}{d\Delta\phi_n} \propto 1 + 2v_n^{\text{obs}} \cos(n\Delta\phi_n).$$

Here $N_{\text{jet}}(p_T, \Delta\phi_n)$ represents the number of jets for a given p_T and $\Delta\phi_n$ selection, where $\Delta\phi_n$ is defined as $\Delta\phi_n = |\Psi_n^{\text{obs}} - \phi|$.

2 ATLAS detector and trigger

The measurement presented in this paper is performed using the ATLAS calorimeter, inner detector, trigger, and data acquisition systems [17]. An extensive software suite [18] is used in the reconstruction and analysis of real and simulated data, in detector operations, and in the trigger and data acquisition systems of the experiment.

The calorimeter system consists of a sampling liquid-argon (LAr) electromagnetic (EM) calorimeter covering $|\eta| < 3.2$, a steel–scintillator sampling hadronic calorimeter covering $|\eta| < 1.7$, LAr hadronic calorimeters covering $1.5 < |\eta| < 3.2$, and two LAr forward calorimeters (FCal) covering $3.2 < |\eta| < 4.9$. The EM calorimeters are segmented longitudinally in shower depth into three layers with an additional presampler layer covering $|\eta| < 1.8$. The hadronic calorimeters have three sampling layers longitudinal in shower depth in $|\eta| < 1.7$ and four sampling layers in $1.5 < |\eta| < 3.2$, with a slight overlap in η .

The inner detector measures charged particles within the pseudorapidity interval $|\eta| < 2.5$ using a combination of silicon pixel detectors, silicon microstrip detectors (SCT), and a straw-tube transition radiation tracker (TRT), all immersed in a 2 T axial magnetic field [17]. Each of the three detectors is composed of a barrel and two symmetric endcap sections. The pixel detector is composed of four layers including the insertable B-layer [19, 20]. The SCT barrel section contains four layers of modules with sensors on both sides, and each endcap consists of nine layers of double-sided modules with radial strips. The TRT contains layers of staggered straws interleaved with the transition radiation material.

² ATLAS uses a right-handed coordinate system with its origin at the nominal interaction point (IP) in the center of the detector, and the z -axis along the beam pipe. The x -axis points from the IP to the center of the LHC ring, and the y -axis points upward. Cylindrical coordinates (r, ϕ) are used in the transverse plane, ϕ being the azimuthal angle around the z -axis. The pseudorapidity is defined in terms of the polar angle θ as $\eta = -\ln \tan(\theta/2)$. The rapidity is defined as $y = 0.5 \ln[(E + p_z)/(E - p_z)]$ where E and p_z are the energy and z -component of the momentum along the beam direction, respectively. Transverse momentum and transverse energy are defined as $p_T = p \sin \theta$ and $E_T = E \sin \theta$, respectively. The angular distance between two objects with relative differences $\Delta\eta$ in pseudorapidity and $\Delta\phi$ in azimuth is given by $\Delta R = \sqrt{(\Delta\eta)^2 + (\Delta\phi)^2}$.

The zero-degree calorimeters (ZDCs) are located symmetrically at $z = \pm 140$ m and cover $|\eta| > 8.3$. The ZDCs use tungsten plates as absorbers, and quartz rods sandwiched between the tungsten plates as the active medium. In Pb+Pb collisions, the ZDCs primarily measure “spectator” neutrons that do not interact hadronically when the incident nuclei collide. A ZDC coincidence trigger is implemented by requiring the pulse height from both ZDCs to be above a threshold which is set to accept the signal corresponding to the energy deposition from a single neutron.

ATLAS uses a two-level trigger system. The first-level trigger is hardware-based and implemented with custom electronics. It is followed by the software-based high-level trigger (HLT) [21].

3 Data and event selection

This analysis uses data from Pb+Pb runs at $\sqrt{s_{\text{NN}}} = 5.02$ TeV collected by the ATLAS detector in 2015 and 2018. Events were selected online by a combination of jet triggers. In the HLT, they require a jet with radius parameter $R = 0.4$ with p_{T} greater than 50, 60, 75, 85, or 100 GeV. The 100 GeV jet trigger sampled the full integrated luminosity of 0.5 nb^{-1} in 2015 and 1.7 nb^{-1} in 2018, while the lower-threshold triggers were prescaled. The data are selected by using each trigger in the region of jet p_{T} for which the HLT triggers are more than 99% efficient, where the efficiency is calculated using reconstructed $R = 0.2$ jets. To populate regions with lower jet p_{T} , events passing minimum-bias (MB) triggers are also included. More details about the jet triggering in heavy-ion collisions can be found in Ref. [22].

The offline event selection requires that events pass both an in-time pileup cut based on the ZDC energy and the total transverse energy in the FCal, and an out-of-time pileup cut based on the number of reconstructed tracks in an event and the total transverse energy in the calorimeter. Here, in-time pileup refers to events with multiple interactions in the same bunch crossing, and out-of-time pileup refers to events in which energy from a previous bunch crossing affects the energy measured in the calorimeter. The pileup rejection cuts remove less than 0.5% of events. Jets selected offline have $|y| < 1.2$ and p_{T} in the range of 63–501 GeV, with jets in the ranges 63–71 GeV and 398–501 GeV used to populate, respectively, the underflow and overflow bins in an unfolding procedure to correct for jet energy scale and resolution effects. The centrality of an event is determined by the sum of transverse energy in the forward calorimeters, $\Sigma E_{\text{T}}^{\text{FCal}}$. Centrality percentiles are determined by separating the MB events into percentiles based on the $\Sigma E_{\text{T}}^{\text{FCal}}$ in each event, ranging from the most central (smallest impact parameter, highest $\Sigma E_{\text{T}}^{\text{FCal}}$) to the most peripheral (largest impact parameter, lowest $\Sigma E_{\text{T}}^{\text{FCal}}$), as described in Ref. [23]. Events are selected with centralities of 0–5%, 5–10%, 10–20%, 20–40%, and 40–60%.

This analysis uses Monte Carlo (MC) simulations to evaluate the performance of the detector and analysis procedure, and to correct the measured distributions for detector effects. The detector response in all MC samples was simulated using GEANT4 [24, 25]. The Pb+Pb MC sample makes use of 7×10^7 dijet events from 5.02 TeV pp collisions simulated by PYTHIA 8 with the A14 set of tuned parameters [26] and the NNPDF2.3LO parton distribution functions [27]. Events from the PYTHIA 8 dijet sample are overlaid with events from a dedicated sample of Pb+Pb data events. This sample was recorded with a combination of the MB trigger and triggers requiring a total energy above 1.5 TeV or 6.5 TeV to enhance the number of central collisions. The overlay procedure combines the PYTHIA 8 and data events during the digitization step of simulation. This MC overlay sample was reweighted on an event-by-event basis such that it has the same $\Sigma E_{\text{T}}^{\text{FCal}}$ distribution as the jet-triggered data sample to better represent the centrality distribution of the data used in this analysis.

4 Analysis procedure

This analysis uses the event-plane method to determine v_n coefficients as described in Ref. [28] and used in previous measurements [29, 30]. The geometry of the initial collision can be characterized by a series of observed event-plane angles, Ψ_n^{obs} ,³ determined by the azimuthal variation of transverse energy in the forward calorimeters. Only the range $|\eta| > 4.0$ of the forward calorimeters is used in this analysis to reduce any bias of the event-plane determination from jets in the FCal. The resolution of the event-plane angles, $\text{Res}\{\Psi_n\}$, is determined by comparing in each event the values calculated in the forward and backward sides of the detector as detailed in Ref. [31]. The resolution is determined for each bin in centrality, and ranges from approximately 0.6–0.9 for Ψ_2 , 0.3–0.6 for Ψ_3 , and 0.2–0.3 for Ψ_4 .

The jet reconstruction procedures follow those used by ATLAS for previous jet measurements in Pb+Pb collisions [2, 10]. Jets are reconstructed using the anti- k_t algorithm [16] implemented in the FastJet software package [32]. Jets with $R = 0.2$ are formed by clustering calorimetric towers of spatial size $\Delta\eta \times \Delta\phi = 0.1 \times \pi/32$. The energies in the towers are obtained by summing the energies of calorimeter cells at the electromagnetic energy scale [33] within the tower boundaries. A background subtraction procedure is applied to estimate within each event the underlying event (UE) average transverse energy density, $\rho(\eta, \phi)$, where the ϕ dependence is due to global azimuthal correlations in the particle production from hydrodynamic flow [31]. The modulation accounts for the contribution to the UE of the second-, third-, and fourth-order azimuthal anisotropy harmonics characterized by values of flow coefficients v_n^{UE} [13]. Any potential residual effect of the azimuthal variation of the underlying event on the jet reconstruction is accounted for by the systematic uncertainties described in Section 5. The UE is also corrected for η - and ϕ -dependent nonuniformities of the detector response by correction factors derived in MB Pb+Pb data.

An iterative procedure is used to remove the impact of jets on the estimated ρ and v_n^{UE} values. The first estimate of the average transverse energy density of the UE, $\rho(\eta)$, is evaluated in 0.1 intervals of η , excluding those which overlap with “seed” jets. In the first subtraction step, the seeds are defined to be a union of $R = 0.2$ jets and $R = 0.4$ track-jets. Track-jets are reconstructed by applying the anti- k_t algorithm with $R = 0.4$ to charged particles with $p_T > 4$ GeV. The $R = 0.2$ jets must pass a cut on the value of the tower energy, while the track-jets are required to have $p_T > 7$ GeV. The background is then subtracted from each tower constituent and jet kinematics are recalculated. After the first iteration, the ρ and v_n values are updated by excluding from the UE determination the regions within $\Delta R = 0.4$ of both the track-jets and the newly reconstructed $R = 0.2$ jets with $p_T > 25$ GeV. The updated ρ and v_n^{UE} values are used to update the jet kinematic properties in the second iteration.

Jet η - and p_T -dependent correction factors derived in simulations are applied to the measured jet energy to correct for the calorimeter energy response [34]. An additional correction based on *in situ* studies of jets recoiling against photons, Z bosons, and jets in other regions of the calorimeter is applied [35]. This calibration is followed by a “cross-calibration” which relates the jet energy scale (JES) of jets reconstructed by the procedure outlined in this section to the JES in 13 TeV pp collisions [36].

So-called “truth jets” are defined in the MC sample before detector simulation by applying the anti- k_t algorithm with $R = 0.2$ to stable particles with a proper lifetime greater than 30 ps, but excluding muons and neutrinos, which do not leave significant energy deposits in the calorimeter.

³ The observed event-plane angles are defined as $\Psi_n = \frac{1}{n} \tan^{-1} \frac{\sum_j E_{T,j} \sin(n\phi_j)}{\sum_j E_{T,j} \cos(n\phi_j)}$ where $E_{T,j}$ is the transverse energy measured in calorimeter tower j of the forward calorimeters.

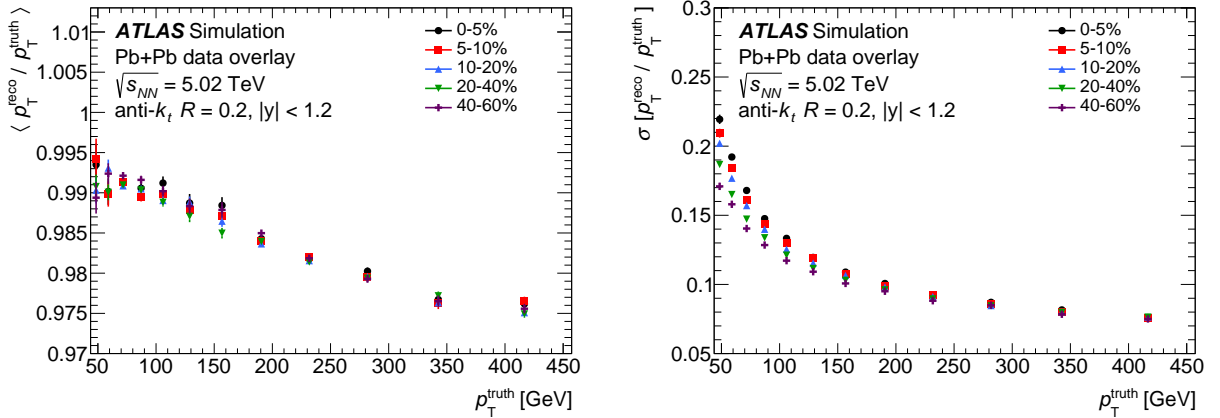


Figure 1: The JES (left) and JER (right) for $R = 0.2$ jets in Pb+Pb collisions as a function of p_T^{truth} for centrality selections of 0–5%, 5–10%, 10–20%, 20–40% and 40–60%.

The JES and jet energy resolution (JER) for $R = 0.2$ jets are shown in Figure 1 as a function of p_T^{truth} . They are derived by matching each truth jet to the closest reconstructed and calibrated jet from the MC overlay sample within an angular distance of $\Delta R = 0.15$. The JES and JER are taken to be the means and standard deviations of the $p_T^{\text{reco}}/p_T^{\text{truth}}$ distributions, respectively. The JES differs from unity by approximately 1% at 70 GeV and 2.5% at 400 GeV; this deviation is due to isolation cuts used in the determination of the jet calibration and is corrected for by the unfolding procedure described below. The JES has no significant centrality dependence. The JER improves with increasing p_T and from central to peripheral collisions. Figure 2 shows the JES and JER for $R = 0.2$ jets as a function of the angle between the jet and the observed second-order event-plane angle. The dependence of the JES on this angle is smaller than its dependence on p_T , with variations up to approximately 0.5% between in-plane and out-of-plane jets. The rapidity range used in this measurement, $|y| < 1.2$, is selected to minimize the JES dependence on the angle with respect to the event plane. The JER also shows a small dependence on the angle between the jet and the second-order event-plane angle, with the resolution of in-plane jets up to 0.5% larger than that for out-of-plane jets.

The jet yield is determined as a function of p_T , centrality, and $\Delta\phi_n$. For each centrality and $\Delta\phi_n$ selection, the jet p_T spectra are unfolded to correct for jet energy scale and resolution effects using a one-dimensional Bayesian unfolding [37] as implemented in the RooUnfold package [38]. The response matrices are filled using spatially matched truth jet and reconstructed jet pairs from the MC overlay sample. The response matrices are reweighted in truth p_T by the ratio of the p_T spectra in data to that in the reconstructed MC sample, such that the p_T spectra in the response matrices better represent those in the data. The reweighting is done separately in each $\Delta\phi_n$ bin, such that the response matrices include the same modulation as seen in the raw data. The unfolding is performed using three iterations, which was found to minimize the combination of the statistical uncertainty and relative bin migration for subsequent iterations. The data are not unfolded to correct for the angular resolution of the jets, which is found to be small compared to the size of the $\Delta\phi_n$ binning.

For each selection in p_T , centrality and harmonic value n , a function is fitted to the unfolded $\Delta\phi_n$ distributions to extract the v_n^{obs} values. The fit function is:

$$A(1 + 2v_n^{\text{obs}} \cos(n\Delta\phi_n))$$

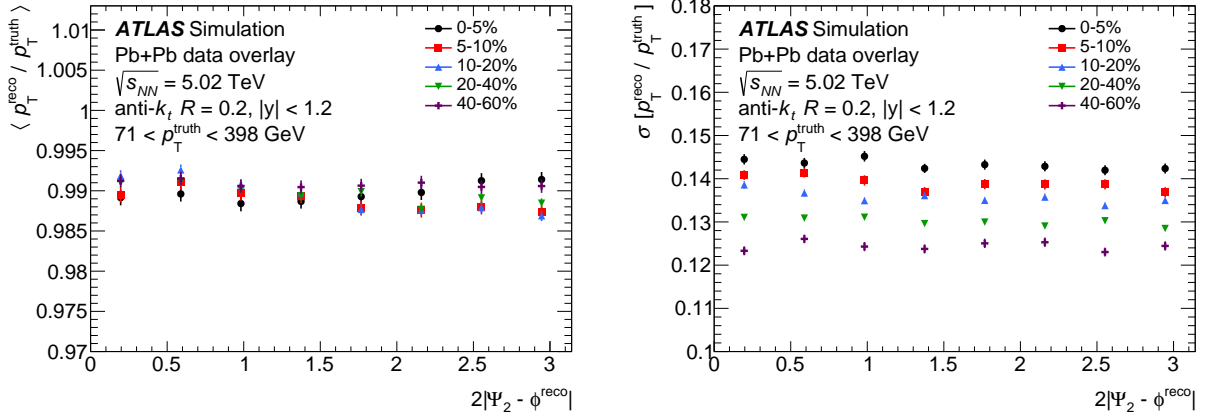


Figure 2: The JES (left) and JER (right) for $R = 0.2$ jets in Pb+Pb collisions as a function of $2|\Psi_2^{\text{obs}} - \phi^{\text{reco}}|$ for centrality selections of 0–5%, 5–10%, 10–20%, 20–40% and 40–60%.

where the overall normalization A and the value of v_n^{obs} are the free parameters in the fitting procedure. The fitted v_n^{obs} values are then corrected for the finite event-plane resolution as described in Ref. [28], where $v_n = v_n^{\text{obs}} / \text{Res}\{\Psi_n\}$. In addition to the v_n measurements differential in jet p_T , the values are also obtained in an inclusive p_T bin for jets with $71 < p_T < 398 \text{ GeV}$, following the same procedure as used in the differential measurement.

5 Systematic uncertainties

The systematic uncertainties in this measurement arise from the JES and JER, the unfolding procedure, and the biasing of the event plane by a forward-produced jet correlated with the jet of interest. The systematic uncertainties presented in this section are given in terms of the absolute change to the measured v_n values. For each uncertainty component the entire analysis procedure is repeated with the variation under consideration and the uncertainty contributions are added in quadrature to obtain the total systematic uncertainty in the measurement.

The systematic uncertainty in the JES has six parts. First, a centrality-independent baseline component is determined from *in situ* studies of the calorimeter response to jets reconstructed with the procedure used in 13 TeV pp collisions [39, 40]. A second, centrality-independent component accounts for the relative energy scale difference between the jet reconstruction procedures used in this analysis and those in 13 TeV pp collisions [36]. Potential inaccuracies in the MC sample in the description of the relative abundances of jets initiated by quarks and gluons and of the calorimetric response to quark and gluon jets are accounted for by the third component. The fourth, centrality-dependent, component accounts for modifications of the parton shower due to quenching and thus possibly a different detector response to jets in Pb+Pb collisions that is not modeled by the MC simulation. It is evaluated by the method used for 2015 and 2011 data [36], which compares the jet p_T measured in the calorimeter and the sum of the transverse momenta of charged particles within the jet, in both the data and MC samples. The charged particles are selected with $p_T > 4 \text{ GeV}$ to remove effects of the UE. The size of the centrality-dependent uncertainty in the JES reaches 1.2% in the most central collisions. An additional, centrality-independent component of 0.5% is included to account for potential year-to-year differences observed between the peripheral Pb+Pb

data taken in 2018 and the pp collision data taken in 2017 which is used for the calibration. The systematic uncertainties from the JES discussed above are derived for $R = 0.4$ jets. The fifth component does not depend on collision centrality and it accounts for the potential difference in uncertainties between $R = 0.4$ and $R = 0.2$ jets. This uncertainty is assessed by comparing the ratio of p_T for matched $R = 0.2$ and $R = 0.4$ jets measured in data and the MC sample. The size of this JES uncertainty is approximately 1%. Each component is varied separately by ± 1 standard deviation in MC samples, applied as a function of p_T and η , and the response matrices are recomputed. The data are then unfolded with the modified matrices. Because the measurement is sensitive only to the relative variation in yields as a function of $\Delta\phi_n$, the measured v_n values are insensitive to these JES uncertainties that do not depend on $\Delta\phi_n$ and therefore these are subdominant uncertainties.

The sixth uncertainty in the JES comes from a potential variation of the scale as a function of the angle between the jet and the event plane. The maximum size of the variations is determined by comparing the jet p_T measured in the calorimeter and the sum of the transverse momenta of charged particles within the jet, as a function of $\Delta\phi_n$, in both the data and MC samples. The v_n due to potential variations in the JES, v_n^{JES} , is determined by modifying the jets in the MC sample for different values of $\Delta\phi_n$ using the comparison of the calorimeter and track measurements and measuring the resulting v_n . The data in each $\Delta\phi_n$ bin are then scaled by $1 + 2v_n^{\text{JES}} \cos(n\Delta\phi_n)$ and fit to extract the systematic variation. Because this measurement is only sensitive to the relative jet yields as a function of $\Delta\phi_n$ and not the overall scale of the yields, systematic variations that vary as a function of $\Delta\phi_n$ will result in a larger uncertainty in the v_n than variations which only depend on the p_T of a jet, such as those described above. Therefore, the uncertainty in the variation of the scale as a function of the angle between the jet and the event plane is the dominant uncertainty in the JES for this measurement.

The uncertainty due to the JER is evaluated by repeating the unfolding procedure with modified response matrices, where an additional contribution is added to the resolution of the reconstructed p_T in the MC sample using a Gaussian smearing procedure. The smearing factor is evaluated using an *in situ* technique in 13 TeV pp data that involves studies of dijet energy balance [41, 42]. Further, an uncertainty is included to account for differences between the tower-based jet reconstruction and the jet reconstruction used in analyses of 13 TeV pp data, as well as differences in calibration procedures. Similarly to the JES, an additional uncertainty is assigned to the JER to account for differences between $R = 0.2$ and $R = 0.4$ jets. The resulting uncertainty from the JER is symmetrized.

The final uncertainty in the JER comes from a potential variation of the resolution as a function of the angle between the jet and the event plane due to the increased size of the UE in-plane compared to out-of-plane. The size of the UE is correlated with the size of the fluctuations of the UE which can lead to too small or too large a subtraction and increase the JER. The v_n due to potential variations in the JER, v_n^{JER} , is determined by adding an additional contribution to the JER of the jets in the MC sample for different values of $\Delta\phi_n$ and measuring the resulting v_n . This additional contribution to the JER is determined by correlating the fluctuations in the UE with the size of the UE in data. The unfolded data in each $\Delta\phi_n$ bin are then scaled by $1 + 2v_n^{\text{JER}} \cos(n\Delta\phi_n)$ and fit to extract the systematic variation. The variations in the JER have a minimal effect on the measured v_n values.

The uncertainty in the unfolding procedure was determined by unfolding the data with response matrices that had not been reweighted to match the p_T spectra in data as described in Section 4 and fitting the unfolded data to obtain new v_n results. The deviation from the nominal unfolding result was symmetrized and taken as the systematic uncertainty contribution.

The uncertainty in the event-plane resolution as determined in Ref. [30] was found to be negligible in comparison with other uncertainties and is not included. However, it is possible for a jet correlated with the jet of interest to bias the event plane if some of its energy is in the FCal. An estimate of the size of this effect was determined from the MC samples. The MC samples were produced without a correlation between the dijets in PYTHIA 8 and the Ψ_n angles in the overlaid data event. Therefore, the measured v_n of jets coming from the PYTHIA 8 event should be zero, and any nonzero v_n values are caused by some events having their event-plane determination biased by a jet from the MC sample. The size of the effect that jets biasing the event-plane angles have on the v_n measured in data is estimated using the v_n values found in the MC sample. The azimuthal modulation of the jet yields in the MC sample is subtracted from that in the unfolded data and the resulting v_n values are taken as the systematic variations.

The total systematic uncertainties of the v_n values and the contributions from each source are summarized in Figure 3. The largest uncertainty for v_2 is the event-plane bias uncertainty, while for v_3 and v_4 the uncertainty in the $\Delta\phi_n$ dependence of the JES is largest. The bin-to-bin variations in the unfolding uncertainty are largely statistical in nature.

Figure 4 shows the systematic uncertainties of the v_n values measured in the inclusive p_T bin of 71–398 GeV. The JES and JER uncertainties are smaller than those in the p_T differential measurements as the variations largely move the jets within the inclusive p_T bin. Similarly, the unfolding uncertainty becomes smaller as the unfolding is a smaller effect for the inclusive bin. The event-plane bias is the largest uncertainty in v_2 , while the JES and event-plane bias are largest uncertainties in v_3 and v_4 .

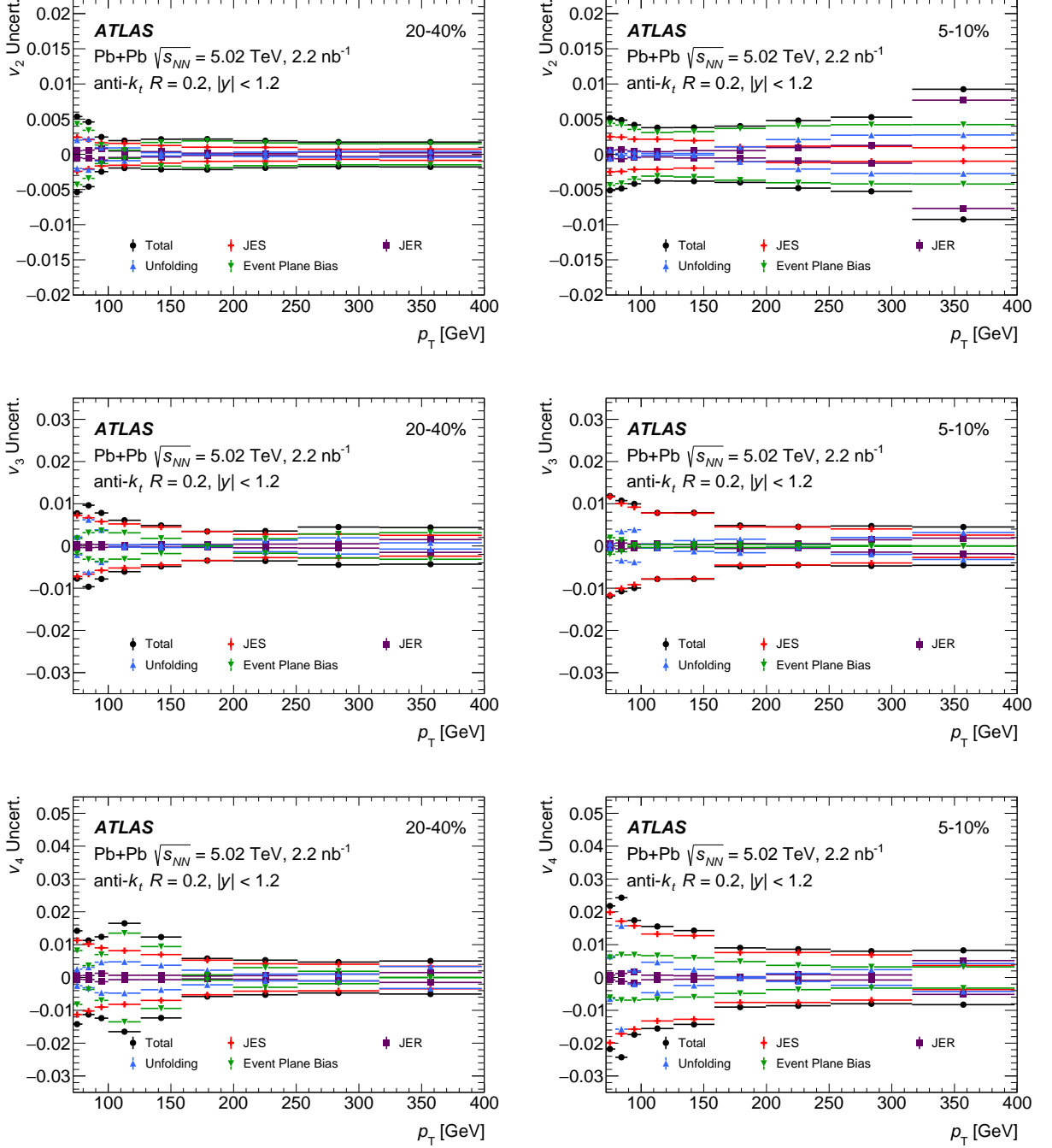


Figure 3: The systematic uncertainties in v_2 (top), v_3 (middle), and v_4 (bottom) for 20–40% (left) and 5–10% (right) centrality Pb+Pb collisions as a function of p_T . Each panel shows the total systematic uncertainty as well as the size of the uncertainty from each of the sources, namely the JES, JER, unfolding, and event-plane bias.

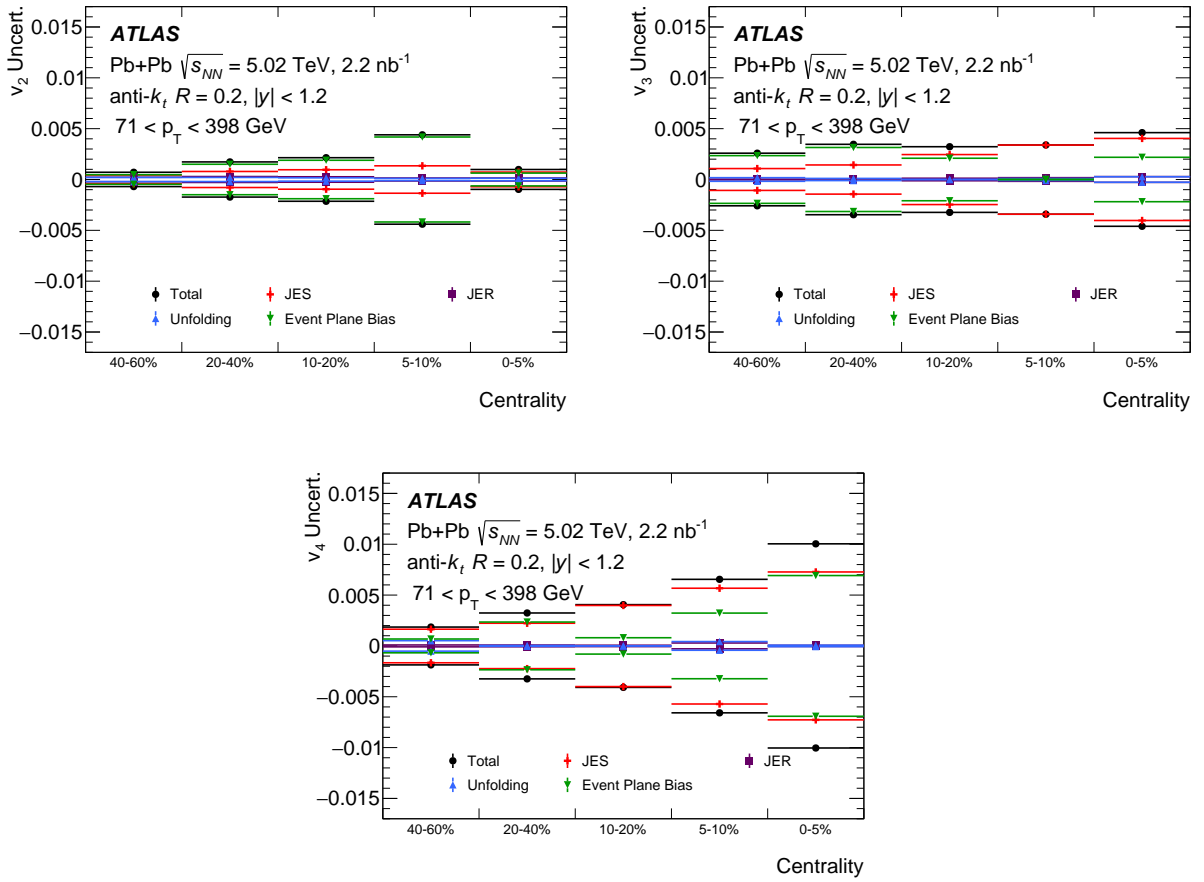


Figure 4: The systematic uncertainties in v_2 , v_3 , and v_4 for $p_T = 71\text{--}398$ GeV jets as a function of centrality. Each panel shows the total systematic uncertainty as well as the size of the uncertainty from each of the sources, namely the JES, JER, unfolding, and event-plane bias.

6 Results

Figure 5 shows an example of the angular distribution of jets with respect to the Ψ_2 , Ψ_3 , and Ψ_4 planes, for jets with $71 < p_T < 79$ GeV in the 10–20% centrality bin. For both the Ψ_2 and Ψ_3 dependence there are more jets in-plane than out-of-plane, although for Ψ_3 the angular dependence is smaller. There is no significant dependence of the jet yield on the angle with respect to Ψ_4 .

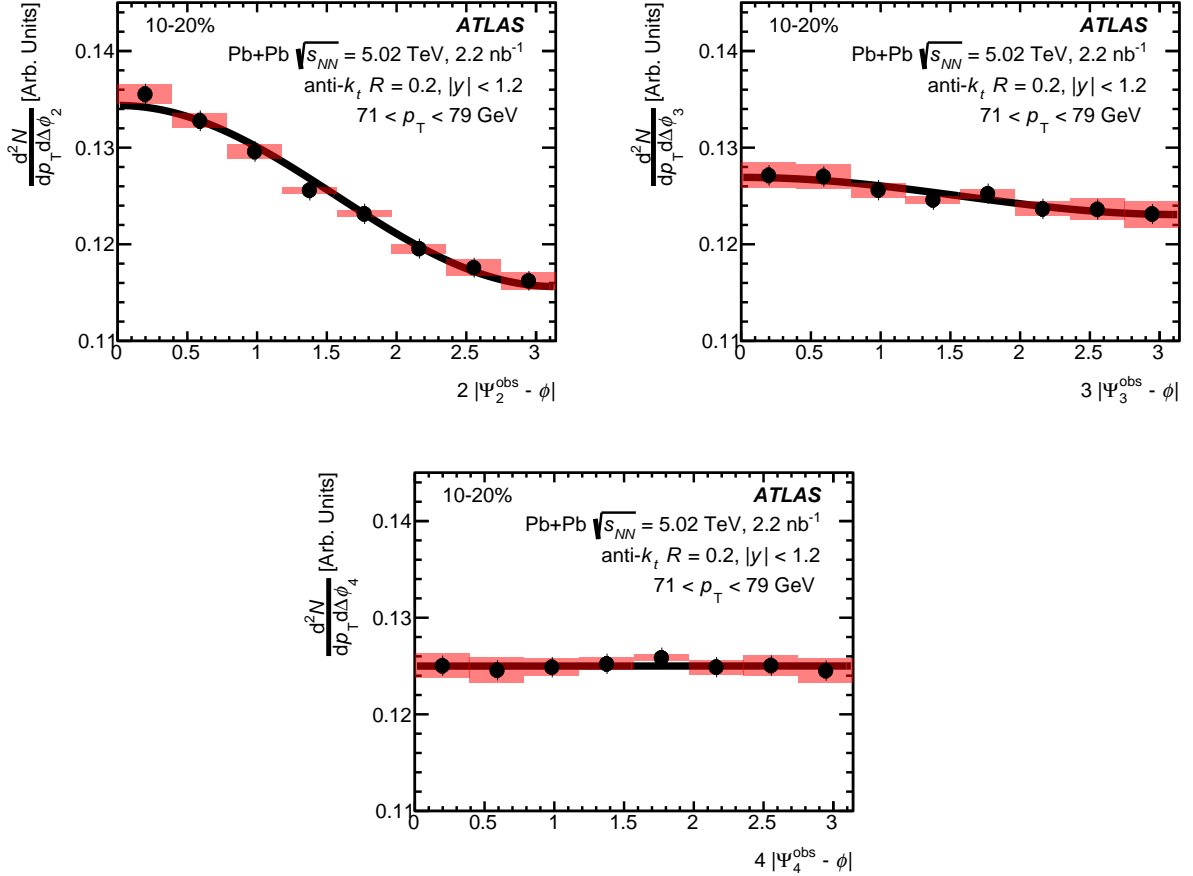


Figure 5: Angular distribution of jets with respect to the Ψ_2^{obs} , Ψ_3^{obs} , and Ψ_4^{obs} planes, $n|\Psi_n^{\text{obs}} - \phi|$, for jets with $71 < p_T < 79$ GeV in the 10–20% centrality bin. The error bars show the statistical uncertainties, which are small compared to the size of the data points, and the boxes show the systematic uncertainties. The black curve shows a fit of the data points to the function $A(1 + 2v_n^{\text{obs}} \cos(n\Delta\phi_n))$.

The v_2 values as a function of centrality for different p_T selections are shown in Figure 6. The v_2 values are consistent with zero in the most central collisions, and positive for all other centrality bins over the full p_T range. For the lower p_T ranges the v_2 values are measured to be as large as 0.05 in mid-central collisions. The v_2 shows a decreasing trend with p_T in mid-central collisions, with a v_2 of approximately 0.01–0.02 for jets with $p_T = 200$ –251 GeV. The value of v_2 decreases for jets which have been shown in previous measurements to be less modified by the QGP, namely jets in peripheral collisions and high- p_T jets. Figure 7 shows the v_2 values for 0–5%, 5–10%, and 20–40% centrality collisions as a function of jet p_T . The value of v_2 decreases from the more peripheral 20–40% collisions to the more central collisions,

where the path-length difference between in-plane and out-of-plane is the smallest. The dependence of the v_2 on p_T in 5–10% and 20–40% collisions shows qualitatively similar behavior.

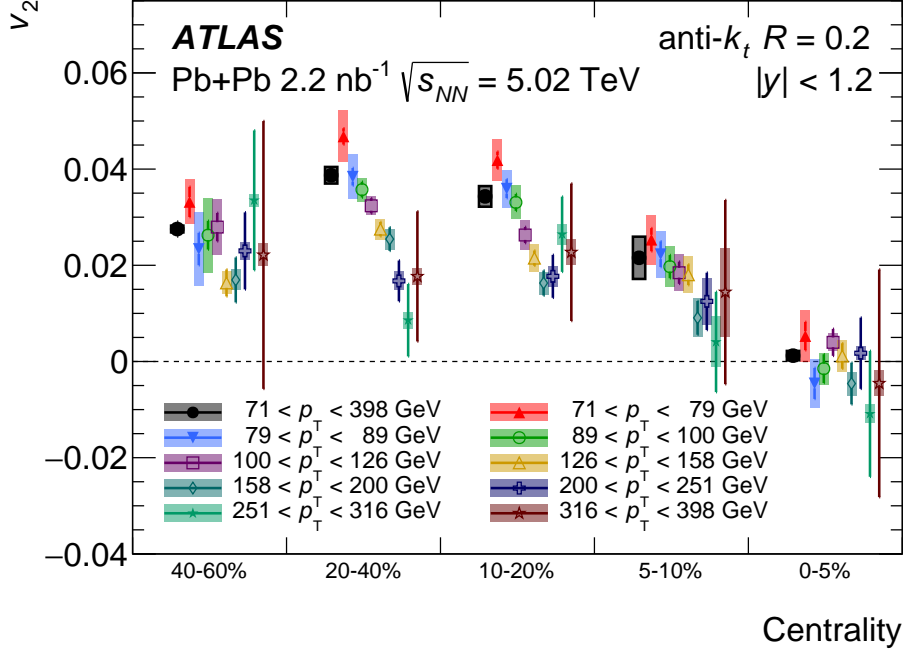


Figure 6: The v_2 values for $R = 0.2$ jets as a function of centrality for jets in several p_T ranges, as indicated in the legend. The error bars represent the statistical error from the fits, while the error boxes represent the systematic uncertainties.

The centrality dependence for the v_2 , v_3 , and v_4 is shown in Figure 8 for the full p_T range of the measurement, 71–398 GeV. The v_2 is nonzero for jets with $p_T < 251$ GeV in all but the most central collisions. The v_3 is positive and on the order of 0.01 for central and mid-central collisions, and consistent with zero in the most peripheral collisions. The difference of the v_3 from 0 is 2.7σ for 20–40%, 3.1σ for 10–20%, 3.3σ for 5–10%, and 1.8σ for 0–5% collisions, where σ is the quadrature sum of the statistical and systematic uncertainties. The value of v_4 is compatible with zero. The measurements of v_3 and v_4 set a limit on the possible impact of initial-state fluctuations on parton energy loss.

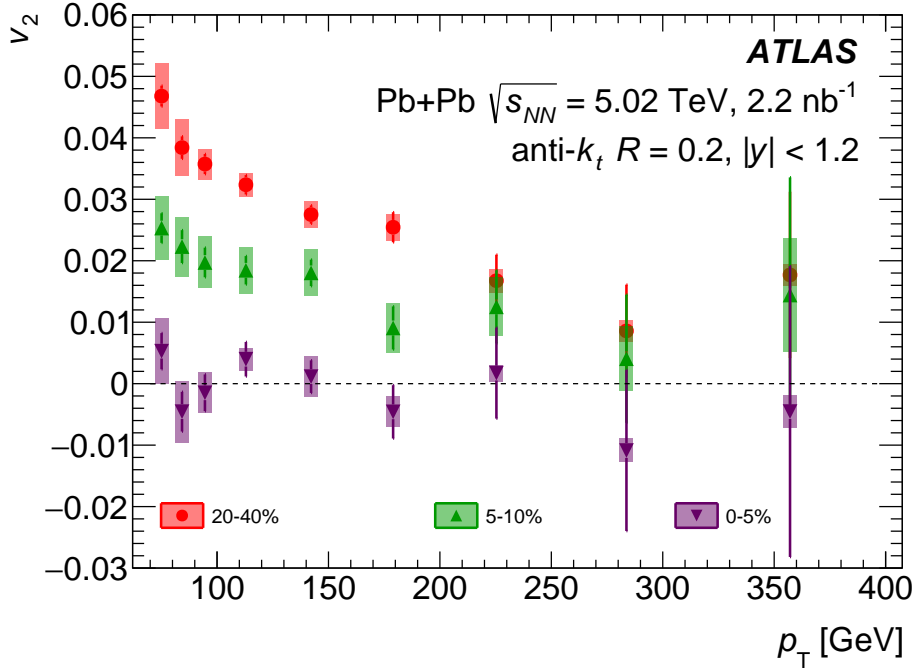


Figure 7: The v_2 values for $R = 0.2$ jets as a function of p_T for 0–5%, 5–10%, and 20–40% centrality collisions. The error bars represent the statistical error from the fits, while the error boxes represent the systematic uncertainties.

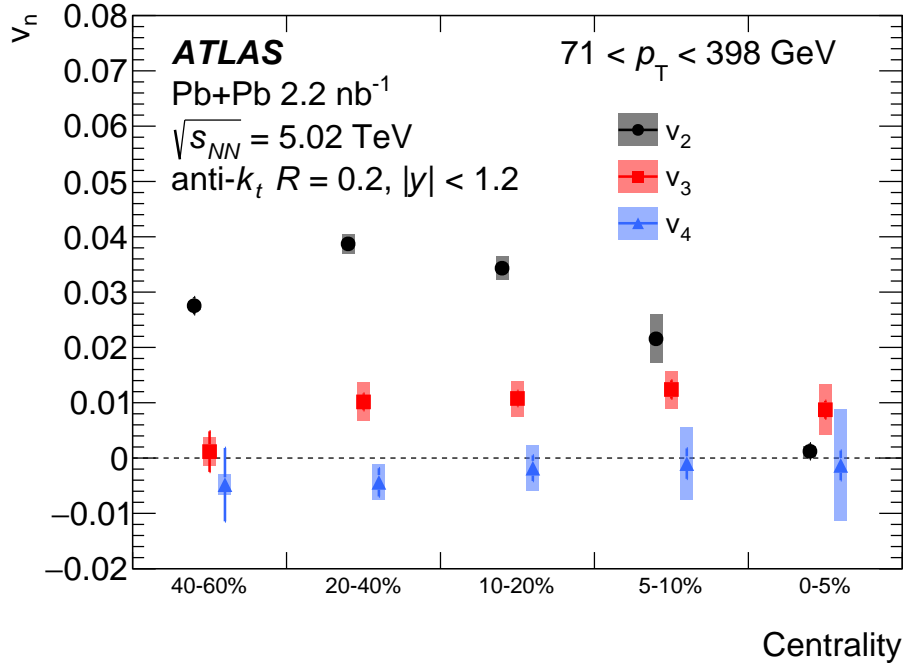


Figure 8: The v_2 , v_3 , and v_4 as a function of centrality for jets with $p_T = 71\text{--}398$ GeV. The error bars represent the statistical error from the fits, while the error boxes represent the systematic uncertainties.

The centrality dependence of the measured v_3 and v_4 values for several p_T ranges are shown in Figure 9. The v_3 shows no significant p_T or centrality dependence, with larger statistical and systematic uncertainties than in the measurement in the inclusive p_T bin. The v_4 measurement is consistent with zero as a function of both p_T and centrality, with larger statistical uncertainties due to the poorer event-plane resolution than that for the second- and third-order event-plane angles.

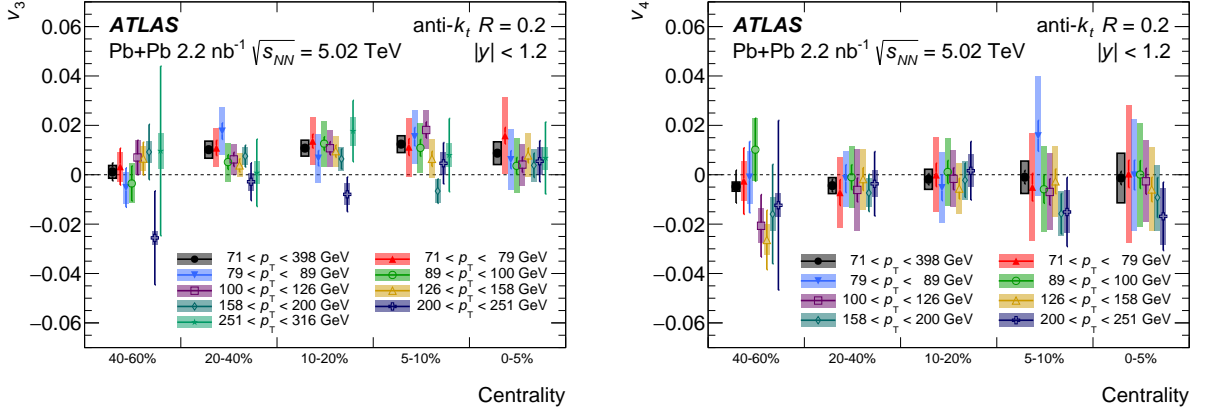


Figure 9: The v_3 (left panel) and v_4 (right panel) of $R = 0.2$ jets as a function of centrality for jets in several p_T ranges, as indicated by the legend. An inclusive bin of $p_T = 71$ – 398 GeV is also shown. The error bars represent the statistical error from the fits, while the error boxes represent the systematic uncertainties.

Figures 10 and 11 compare the results of this measurement with the jet v_2 measurements at $\sqrt{s_{NN}} = 2.76$ TeV for fully reconstructed jets from Ref. [10] and charged-particle jets from Ref. [11] for the 10–20% and 20–40% centrality bins. The measurement shows good agreement with the previous results, with no significant evidence of a dependence of the v_n values on the collision energy. The v_2 and v_3 of charged particles from Ref. [12] is also shown. The results show a qualitatively similar p_T dependence, with the charged-particle v_n distribution shifted to lower p_T . This is consistent with the expectation that high- p_T charged particles are likely produced from jets at a higher p_T . This result improves on both the p_T reach and precision of previous measurements of high- p_T jet v_n .

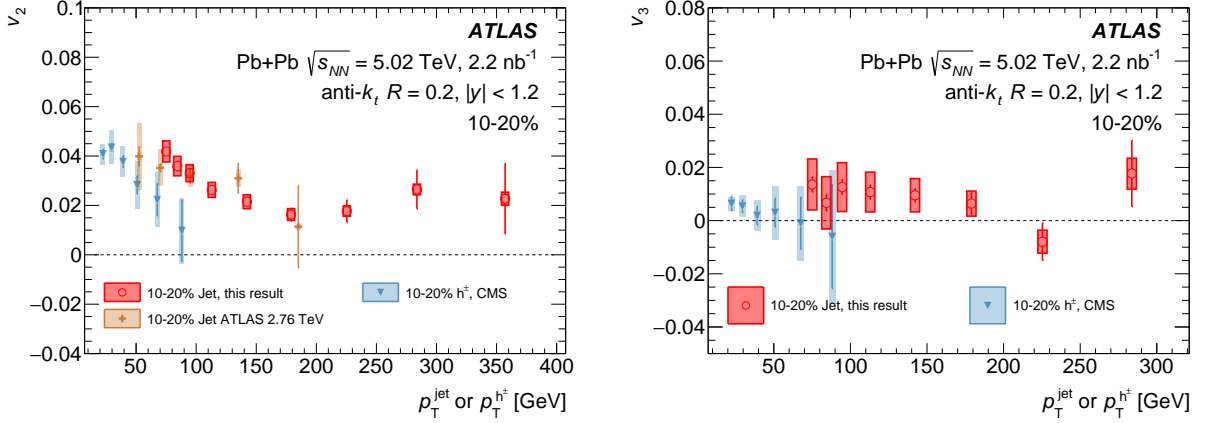


Figure 10: The v_2 and v_3 as a function of p_T for jets in 10–20% centrality collisions in this measurement (red circles) compared with the v_2 of jets in $\sqrt{s_{NN}} = 2.76$ TeV Pb+Pb collisions from Ref. [10] (brown crosses) and the v_2 and v_3 of charged particles in $\sqrt{s_{NN}} = 5.02$ TeV Pb+Pb collisions from Ref. [12] (blue triangles).

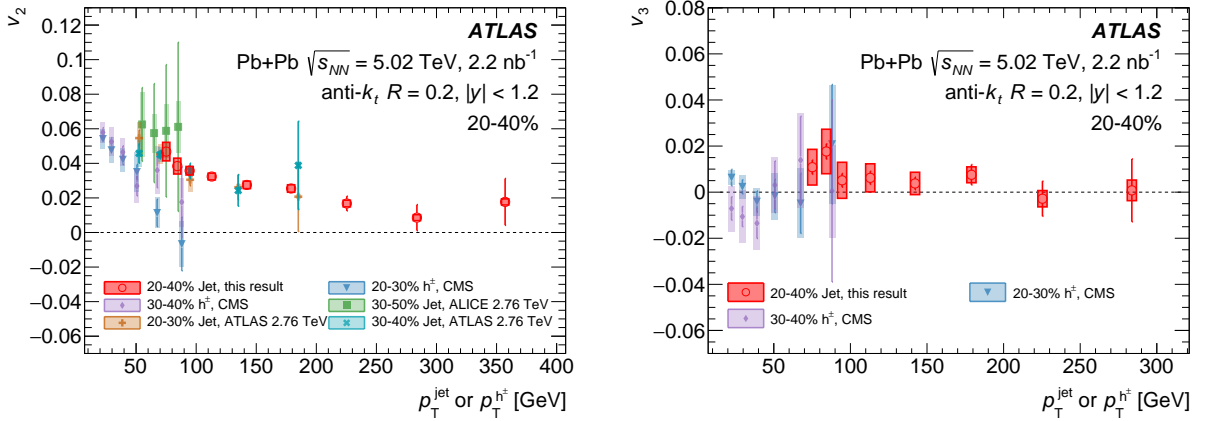


Figure 11: The v_2 and v_3 as a function of p_T for jets in 20–40% centrality collisions in this measurement (red circles) compared with the v_2 of jets in $\sqrt{s_{NN}} = 2.76$ TeV Pb+Pb collisions from Ref. [10] for 20–30% centrality collisions (brown crosses) and 30–40% centrality collisions (cyan X markers) and from Ref. [11] for 30–50% centrality collisions (green squares) and the v_2 and v_3 of charged particles in $\sqrt{s_{NN}} = 5.02$ TeV Pb+Pb collisions from Ref. [12] for 20–30% centrality collisions (blue triangles) and 30–40% centrality collisions (purple diamonds).

Figure 12 shows the v_2 and v_3 as a function of p_T compared with theoretical calculations: LIDO from Ref. [43] and the Linear Boltzmann Transport (LBT) model from Refs. [44–46]. LIDO is a transport model including both elastic jet–medium collisions and medium-induced radiative processes, as well as a simple model for the response of the medium. The v_n is computed with an event-by-event model of the QGP medium [47]. The calculations are performed using two values for the jet–medium coupling cutoff parameter: $\mu = 1.5$ and $\mu = 2.0$. This parameter is related to the strength of the coupling between the jet and the medium, where a smaller μ value corresponds to a larger coupling [43]. The choice of μ values is motivated by comparisons with measurements of jet quenching. The LIDO model describes the v_2 and v_3 well, with the data favoring the $\mu = 2.0$ calculation at higher p_T and the $\mu = 1.5$ calculation at lower p_T . The LBT model simulates the propagation of jet shower and thermal recoil partons in the same framework

and includes the effect of the jet-induced medium particles in the reconstruction of the final jets. The model uses event-by-event hydrodynamics as described in Ref. [48]. The calculation is shown using the event-plane method (EP), which does not include soft hadron fluctuations, and the scalar-product method (SP), which does include soft hadron fluctuations [49]. The LBT model agrees with the size of the v_3 within the uncertainties of this measurement, but does not describe the variation of v_2 as a function of p_T .

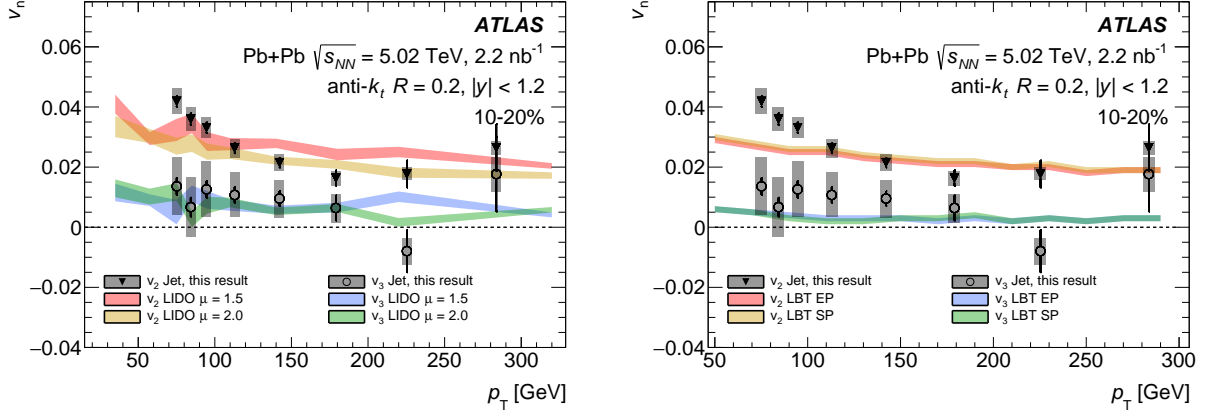


Figure 12: The v_2 and v_3 for jets in 10–20% centrality collisions compared with theoretical calculations using the LIDO [43] (left) and LBT [44–46] (right) models. The LIDO calculation is shown for two values of the jet–medium coupling cutoff parameter, μ . The LBT calculation is shown using the event-plane method (EP) and the scalar-product method (SP).

It is interesting to compare the actual jet yields in-plane versus out-of-plane to study the angular distribution of jets without imposing the $\cos(n\Delta\phi_n)$ shape modulation on the data. The ratio of the jet yields in the most in-plane bin, $n\Delta\phi_n < \pi/8$, to the most out-of-plane bin, $n\Delta\phi_n > 7\pi/8$, is constructed:

$$R_n^{\max} \equiv \frac{d^2N}{dp_T d\Delta\phi_n} \Big|_{n\Delta\phi_n > 7\pi/8} / \frac{d^2N}{dp_T d\Delta\phi_n} \Big|_{n\Delta\phi_n < \pi/8}.$$

These yields must be corrected for the finite event-plane resolution, which is done by assuming that the variation in $\Delta\phi_n$ is dominated by the $\cos(n\Delta\phi_n)$ modulation such that

$$\frac{d^2N_{\text{jet}}^{\text{corr}}}{dp_T d\Delta\phi_n} = \frac{d^2N_{\text{jet}}^{\text{obs}}}{dp_T d\Delta\phi_n} \left(\frac{1 + 2v_n \cos n\Delta\phi_n}{1 + 2v_n^{\text{obs}} \cos n\Delta\phi_n} \right).$$

The ratio is further corrected for the effects of the finite bin width by assuming a $\cos(n\Delta\phi_n)$ modulation within each bin, and calculating the yields at $n\Delta\phi_n = 0$ and $n\Delta\phi_n = \pi$, and taking the ratio of these values. A similar method was used in Ref. [10]. This ratio, for $n = 2$ and 3 , is shown in Figure 13. A purely $\cos(n\Delta\phi_n)$ modulation would cause R_n^{\max} to be $1 - 4v_n/(1 + 2v_n)$ and these calculated values are compared with the R_n^{\max} values. No deviation from the $\cos(n\Delta\phi_n)$ modulation is observed.

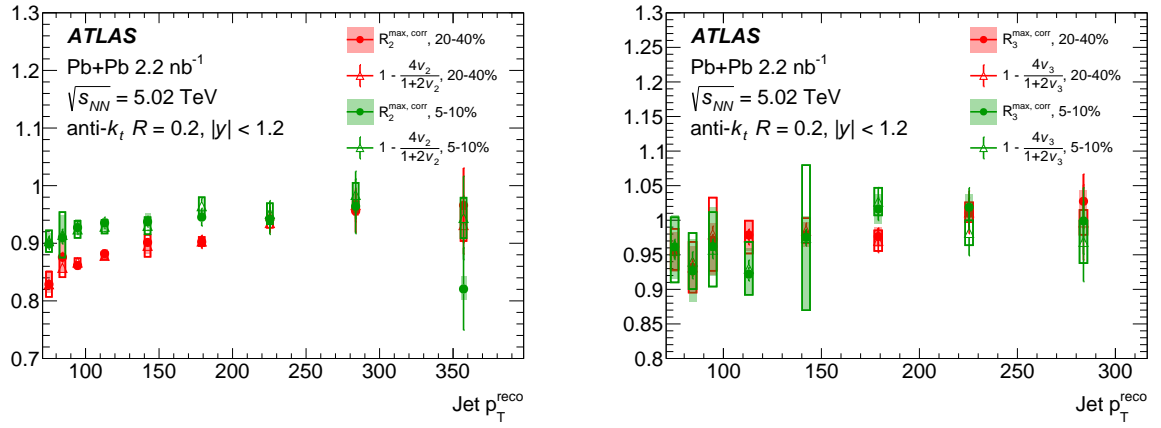


Figure 13: R_n^{max} for $n = 2$ (left) and $n = 3$ (right) as a function of p_T (filled circles). Also shown is $1 - 4v_n/(1 + 2v_n)$ (open circles). The values are shown for 5–10% (green) and 20–40% (red) collisions.

7 Conclusion

The azimuthal variation of jet quenching is measured in 2.2 nb^{-1} of Pb+Pb collisions at 5.02 TeV, using the event-plane method to extract the v_n coefficients of jets. The data were collected with the ATLAS detector at the LHC. The v_2 is found to be consistent with zero in the most central collisions, with values up to 0.05 in mid-central collisions, and decreasing with increasing p_T . A first measurement of v_3 and v_4 of jets is presented. The value of v_3 is found to be significantly above zero in mid-central collisions, with a value of approximately 0.01 for central and mid-central collisions. The p_T -differential measurement of v_3 shows no significant p_T or centrality dependence, while v_4 is everywhere consistent with zero. The measured values are consistent with previous measurements of jet and high- p_T hadron v_n , and improve on both the p_T reach and precision of these previous results. The positive v_2 values in all but the most azimuthally symmetric collisions show the relationship between collision geometry and parton energy loss. Further, the measurements of v_3 and v_4 will help set limits on the impact of initial-state fluctuations on energy loss. These measurements can be used to constrain models of the path-length dependence of jet quenching.

Acknowledgments

We thank CERN for the very successful operation of the LHC, as well as the support staff from our institutions without whom ATLAS could not be operated efficiently.

We acknowledge the support of ANPCyT, Argentina; YerPhI, Armenia; ARC, Australia; BMFWF and FWF, Austria; ANAS, Azerbaijan; SSTC, Belarus; CNPq and FAPESP, Brazil; NSERC, NRC and CFI, Canada; CERN; ANID, Chile; CAS, MOST and NSFC, China; Minciencias, Colombia; MSMT CR, MPO CR and VSC CR, Czech Republic; DNRF and DNSRC, Denmark; IN2P3-CNRS and CEA-DRF/IRFU, France; SRNSFG, Georgia; BMBF, HGF and MPG, Germany; GSRI, Greece; RGC and Hong Kong SAR, China; ISF and Benozio Center, Israel; INFN, Italy; MEXT and JSPS, Japan; CNRST, Morocco; NWO, Netherlands; RCN, Norway; MEiN, Poland; FCT, Portugal; MNE/IFA, Romania; JINR; MES of Russia and NRC KI, Russian Federation; MESTD, Serbia; MSSR, Slovakia; ARRS and MIZŠ, Slovenia; DSI/NRF, South Africa; MICINN, Spain; SRC and Wallenberg Foundation, Sweden; SERI, SNSF and Cantons of Bern and Geneva, Switzerland; MOST, Taiwan; TAEK, Turkey; STFC, United Kingdom; DOE and NSF, United States of America. In addition, individual groups and members have received support from BCKDF, CANARIE, Compute Canada and CRC, Canada; COST, ERC, ERDF, Horizon 2020 and Marie Skłodowska-Curie Actions, European Union; Investissements d’Avenir Labex, Investissements d’Avenir IDEX and ANR, France; DFG and AvH Foundation, Germany; Herakleitos, Thales and Aristeia programmes co-financed by EU-ESF and the Greek NSRF, Greece; BSF-NSF and GIF, Israel; Norwegian Financial Mechanism 2014-2021, Norway; NCN and NAWA, Poland; La Caixa Banking Foundation, CERCA Programme Generalitat de Catalunya and PROMETEO and GenT Programmes Generalitat Valenciana, Spain; Göran Gustafssons Stiftelse, Sweden; The Royal Society and Leverhulme Trust, United Kingdom.

The crucial computing support from all WLCG partners is acknowledged gratefully, in particular from CERN, the ATLAS Tier-1 facilities at TRIUMF (Canada), NDGF (Denmark, Norway, Sweden), CC-IN2P3 (France), KIT/GridKA (Germany), INFN-CNAF (Italy), NL-T1 (Netherlands), PIC (Spain), ASGC (Taiwan), RAL (UK) and BNL (USA), the Tier-2 facilities worldwide and large non-WLCG resource providers. Major contributors of computing resources are listed in Ref. [50].

References

- [1] W. Busza, K. Rajagopal, and W. van der Schee, *Heavy Ion Collisions: The Big Picture, and the Big Questions*, *Ann. Rev. Nucl. Part. Sci.* **68** (2018) 339, arXiv: [1802.04801 \[hep-ph\]](#).
- [2] ATLAS Collaboration, *Measurement of the nuclear modification factor for inclusive jets in Pb+Pb collisions at $\sqrt{s_{NN}} = 5.02$ TeV with the ATLAS detector*, *Phys. Lett. B* **790** (2019) 108, arXiv: [1805.05635 \[nucl-ex\]](#).
- [3] CMS Collaboration, *First measurement of large area jet transverse momentum spectra in heavy-ion collisions*, *JHEP* **05** (2021) 284, arXiv: [2102.13080 \[hep-ex\]](#).
- [4] X.-N. Wang, *Jet quenching and azimuthal anisotropy of large p_T spectra in noncentral high-energy heavy-ion collisions*, *Phys. Rev. C* **63** (2001) 054902, arXiv: [nucl-th/0009019](#).
- [5] M. Gyulassy, I. Vitev, and X.-N. Wang, *High p_T Azimuthal Asymmetry in Noncentral A+A at RHIC*, *Phys. Rev. Lett.* **86** (2001) 2537, arXiv: [nucl-th/0012092](#).
- [6] E. V. Shuryak, *Azimuthal asymmetry at large p_t seem to be too large for a pure “jet quenching”*, *Phys. Rev. C* **66** (2002) 027902, arXiv: [nucl-th/0112042](#).
- [7] U. Heinz and R. Snellings, *Collective flow and viscosity in relativistic heavy-ion collisions*, *Ann. Rev. Nucl. Part. Sci.* **63** (2013) 123, arXiv: [1301.2826 \[nucl-th\]](#).
- [8] PHENIX Collaboration, *Azimuthal anisotropy of π^0 and η mesons in Au + Au collisions at $\sqrt{s_{NN}} = 200$ GeV*, *Phys. Rev. C* **88** (2013) 064910, arXiv: [1309.4437 \[nucl-ex\]](#).
- [9] STAR Collaboration, *Azimuthal anisotropy in Au+Au collisions at $\sqrt{s_{NN}} = 200$ GeV*, *Phys. Rev. C* **72** (2005) 014904.
- [10] ATLAS Collaboration, *Measurement of the Azimuthal Angle Dependence of Inclusive Jet Yields in Pb+Pb Collisions at $\sqrt{s_{NN}} = 2.76$ TeV with the ATLAS Detector*, *Phys. Rev. Lett.* **111** (2013) 152301, arXiv: [1306.6469 \[hep-ex\]](#).
- [11] ALICE Collaboration, *Azimuthal anisotropy of charged jet production in $\sqrt{s_{NN}}=2.76$ TeV Pb-Pb collisions*, *Phys. Lett. B* **753** (2016) 511.
- [12] CMS Collaboration, *Azimuthal anisotropy of charged particles with transverse momentum up to 100 GeV/c in PbPb collisions at $\sqrt{s_{NN}}=5.02$ TeV*, *Phys. Lett. B* **776** (2018) 195, arXiv: [1702.00630 \[hep-ex\]](#).
- [13] ATLAS Collaboration, *Measurement of the azimuthal anisotropy of charged particles produced in $\sqrt{s_{NN}} = 5.02$ TeV Pb+Pb collisions with the ATLAS detector*, *Eur. Phys. J. C* **78** (2018) 997, arXiv: [1808.03951 \[nucl-ex\]](#).
- [14] J. Noronha-Hostler, B. Betz, J. Noronha, and M. Gyulassy, *Event-by-Event Hydrodynamics + Jet Energy Loss: A Solution to the $R_{AA} \otimes v_2$ Puzzle*, *Phys. Rev. Lett.* **116** (2016) 252301, arXiv: [1602.03788 \[nucl-th\]](#).
- [15] J. Noronha-Hostler et al., *Cumulants and nonlinear response of high p_T harmonic flow at $\sqrt{s_{NN}} = 5.02$ TeV*, *Phys. Rev. C* **95** (2017) 044901, arXiv: [1609.05171 \[nucl-th\]](#).

- [16] M. Cacciari, G. P. Salam, and G. Soyez, *The anti- k_t jet clustering algorithm*, *JHEP* **04** (2008) 063, arXiv: [0802.1189 \[hep-ph\]](#).
- [17] ATLAS Collaboration, *The ATLAS Experiment at the CERN Large Hadron Collider*, *JINST* **3** (2008) S08003.
- [18] ATLAS Collaboration, *The ATLAS Collaboration Software and Firmware*, ATL-SOFT-PUB-2021-001, 2021, URL: <https://cds.cern.ch/record/2767187>.
- [19] ATLAS Collaboration, *ATLAS Insertable B-Layer: Technical Design Report*, ATLAS-TDR-19; CERN-LHCC-2010-013, 2010, URL: <https://cds.cern.ch/record/1291633>, Addendum: ATLAS-TDR-19-ADD-1; CERN-LHCC-2012-009, 2012, URL: <https://cds.cern.ch/record/1451888>.
- [20] B. Abbott et al., *Production and integration of the ATLAS Insertable B-Layer*, *JINST* **13** (2018) T05008, arXiv: [1803.00844 \[physics.ins-det\]](#).
- [21] ATLAS Collaboration, *Operation of the ATLAS trigger system in Run 2*, *JINST* **15** (2020) P10004, arXiv: [2007.12539 \[hep-ex\]](#).
- [22] ATLAS Collaboration, *Trigger Menu in 2018*, ATL-DAQ-PUB-2019-001, 2019, URL: <https://cds.cern.ch/record/2693402>.
- [23] ATLAS Collaboration, *Measurement of longitudinal flow decorrelations in Pb+Pb collisions at $\sqrt{s_{NN}} = 2.76$ and 5.02 TeV with the ATLAS detector*, *Eur. Phys. J. C* **78** (2018) 142, arXiv: [1709.02301 \[hep-ex\]](#).
- [24] S. Agostinelli et al., *GEANT4—a simulation toolkit*, *Nucl. Instrum. Meth. A* **506** (2003) 250.
- [25] ATLAS Collaboration, *The ATLAS Simulation Infrastructure*, *Eur. Phys. J. C* **70** (2010) 823, arXiv: [1005.4568 \[physics.ins-det\]](#).
- [26] ATLAS Collaboration, ATLAS-PHYS-PUB-2014-021, <https://cds.cern.ch/record/1966419>.
- [27] R. D. Ball et al., *Parton distributions with LHC data*, *Nucl. Phys. B* **867** (2013) 244, arXiv: [1207.1303 \[hep-ph\]](#).
- [28] A. M. Poskanzer and S. A. Voloshin, *Methods for analyzing anisotropic flow in relativistic nuclear collisions*, *Phys. Rev. C* **58** (3 1998) 1671.
- [29] ATLAS Collaboration, *Prompt and non-prompt J/ψ elliptic flow in Pb+Pb collisions at $\sqrt{s_{NN}} = 5.02$ TeV with the ATLAS detector*, *Eur. Phys. J. C* **78** (2018) 784, arXiv: [1807.05198 \[hep-ex\]](#).
- [30] ATLAS Collaboration, *Measurement of azimuthal anisotropy of muons from charm and bottom hadrons in Pb+Pb collisions at $\sqrt{s_{NN}} = 5.02$ TeV with the ATLAS detector*, *Phys. Lett. B* **807** (2020) 135595, arXiv: [2003.03565 \[hep-ex\]](#).
- [31] ATLAS Collaboration, *Measurement of the azimuthal anisotropy of charged particles produced in $\sqrt{s_{NN}} = 5.02$ TeV Pb+Pb collisions with the ATLAS detector*, *Eur. Phys. J. C* **78** (2018) 997, arXiv: [1808.03951 \[hep-ex\]](#).
- [32] M. Cacciari, G. P. Salam, and G. Soyez, *FastJet user manual*, *Eur. Phys. J. C* **72** (2012) 1896, arXiv: [1111.6097 \[hep-ph\]](#).
- [33] ATLAS Collaboration, *Jet energy measurement with the ATLAS detector in proton–proton collisions at $\sqrt{s} = 7$ TeV*, *Eur. Phys. J. C* **73** (2013) 2304, arXiv: [1112.6426 \[hep-ex\]](#).

- [34] ATLAS Collaboration, *Jet energy measurement and its systematic uncertainty in proton-proton collisions at $\sqrt{s} = 7$ TeV with the ATLAS detector*, *Eur. Phys. J. C* **75** (2015) 17, arXiv: [1406.0076 \[hep-ex\]](#).
- [35] ATLAS Collaboration, *Measurement of photon-jet transverse momentum correlations in 5.02 TeV Pb+Pb and pp collisions with ATLAS*, *Phys. Lett. B* **789** (2019) 167, arXiv: [1809.07280 \[hep-ex\]](#).
- [36] ATLAS Collaboration, *Jet energy scale and its uncertainty for jets reconstructed using the ATLAS heavy ion jet algorithm*, ATLAS-CONF-2015-016, 2015, URL: <https://cds.cern.ch/record/2008677>.
- [37] G. D'Agostini, *A Multidimensional unfolding method based on Bayes' theorem*, *Nucl. Instrum. Meth. A* **362** (1995) 487.
- [38] T. Auye, *Unfolding algorithms and tests using RooUnfold*, 2011, arXiv: [1105.1160 \[physics.data-an\]](#).
- [39] ATLAS Collaboration, *Jet energy measurement with the ATLAS detector in proton-proton collisions at $\sqrt{s} = 7$ TeV*, *Eur. Phys. J. C* **73** (2013) 2304, arXiv: [1112.6426 \[hep-ex\]](#).
- [40] ATLAS Collaboration, *Jet energy scale measurements and their systematic uncertainties in proton-proton collisions at $\sqrt{s} = 13$ TeV with the ATLAS detector*, *Phys. Rev. D* **96** (2017) 072002, arXiv: [1703.09665 \[hep-ex\]](#).
- [41] ATLAS Collaboration, *Jet energy resolution in proton-proton collisions at $\sqrt{s} = 7$ TeV recorded in 2010 with the ATLAS detector*, *Eur. Phys. J. C* **73** (2013) 2306, arXiv: [1210.6210 \[hep-ex\]](#).
- [42] ATLAS Collaboration, *Determination of jet calibration and energy resolution in proton-proton collisions at $\sqrt{s} = 8$ TeV using the ATLAS detector*, *Eur. Phys. J. C* **80** (2020) 1104, arXiv: [1910.04482 \[hep-ex\]](#).
- [43] W. Ke and X.-N. Wang, *QGP modification to single inclusive jets in a calibrated transport model*, *JHEP* **05** (2021) 041, arXiv: [2010.13680 \[hep-ph\]](#).
- [44] Y. He, T. Luo, X.-N. Wang, and Y. Zhu, *Linear Boltzmann transport for jet propagation in the quark-gluon plasma: Elastic processes and medium recoil*, *Phys. Rev. C* **91** (5 2015) 054908.
- [45] Y. He et al., *Interplaying mechanisms behind single inclusive jet suppression in heavy-ion collisions*, *Phys. Rev. C* **99** (2019) 054911.
- [46] Y. He et al., *E-by-e jet suppression, anisotropy, medium response and hard-soft tomography*, *Nucl. Phys. A* **982** (2019) 635, ed. by F. Antinori et al., arXiv: [1811.08975 \[nucl-th\]](#).
- [47] J. E. Bernhard, J. S. Moreland, and S. A. Bass, *Bayesian estimation of the specific shear and bulk viscosity of quark-gluon plasma*, *Nature Physics* **15** (2019) 1113.
- [48] L.-G. Pang, H. Petersen, and X.-N. Wang, *Pseudorapidity distribution and decorrelation of anisotropic flow within the open-computing-language implementation CLVisc hydrodynamics*, *Phys. Rev. C* **97** (6 2018) 064918.
- [49] Star Collaboration, *Elliptic flow from two- and four-particle correlations in Au+Au collisions at $\sqrt{s_{NN}} = 130$ GeV*, *Phys. Rev. C* **66** (3 2002) 034904.

[50] ATLAS Collaboration, *ATLAS Computing Acknowledgements*, ATL-SOFT-PUB-2021-003,
URL: <https://cds.cern.ch/record/2776662>.

The ATLAS Collaboration

G. Aad⁹⁹, B. Abbott¹²⁵, D.C. Abbott¹⁰⁰, A. Abed Abud³⁵, K. Abeling⁵², D.K. Abhayasinghe⁹², S.H. Abidi²⁸, A. Aboulhorma^{34e}, H. Abramowicz¹⁵⁸, H. Abreu¹⁵⁷, Y. Abulaiti¹²², A.C. Abusleme Hoffman^{143a}, B.S. Acharya^{65a,65b,n}, B. Achkar⁵², L. Adam⁹⁷, C. Adam Bourdarios⁴, L. Adamczyk^{82a}, L. Adamek¹⁶³, S.V. Addepalli²⁵, J. Adelman¹¹⁷, A. Adiguzel^{11c,y}, S. Adorni⁵³, T. Adye¹⁴⁰, A.A. Affolder¹⁴², Y. Afik³⁵, C. Agapopoulou⁶³, M.N. Agaras¹³, J. Agarwala^{69a,69b}, A. Aggarwal¹¹⁵, C. Agheorghiesei^{26c}, J.A. Aguilar-Saavedra^{136f,136a,x}, A. Ahmad³⁵, F. Ahmadov⁷⁸, W.S. Ahmed¹⁰¹, X. Ai⁴⁵, G. Aielli^{72a,72b}, I. Aizenberg¹⁷⁶, S. Akatsuka⁸⁴, M. Akbiyik⁹⁷, T.P.A. Åkesson⁹⁵, A.V. Akimov¹⁰⁸, K. Al Khoury³⁸, G.L. Alberghi^{22b}, J. Albert¹⁷², P. Albicocco⁵⁰, M.J. Alconada Verzini⁸⁷, S. Alderweireldt⁴⁹, M. Aleksa³⁵, I.N. Aleksandrov⁷⁸, C. Alexa^{26b}, T. Alexopoulos⁹, A. Alfonsi¹¹⁶, F. Alfonsi^{22b}, M. Alhroob¹²⁵, B. Ali¹³⁸, S. Ali¹⁵⁵, M. Aliev¹⁶², G. Alimonti^{67a}, C. Allaire³⁵, B.M.M. Allbrooke¹⁵³, P.P. Allport²⁰, A. Aloisio^{68a,68b}, F. Alonso⁸⁷, C. Alpigiani¹⁴⁵, E. Alunno Camelia^{72a,72b}, M. Alvarez Estevez⁹⁶, M.G. Alviggi^{68a,68b}, Y. Amaral Coutinho^{79b}, A. Ambler¹⁰¹, L. Ambroz¹³¹, C. Amelung³⁵, D. Amidei¹⁰³, S.P. Amor Dos Santos^{136a}, S. Amoroso⁴⁵, K.R. Amos¹⁷⁰, C.S. Amrouche⁵³, V. Ananiev¹³⁰, C. Anastopoulos¹⁴⁶, N. Andari¹⁴¹, T. Andeen¹⁰, J.K. Anders¹⁹, S.Y. Andrean^{44a,44b}, A. Andreazza^{67a,67b}, S. Angelidakis⁸, A. Angerami³⁸, A.V. Anisenkov^{118b,118a}, A. Annovi^{70a}, C. Antel⁵³, M.T. Anthony¹⁴⁶, E. Antipov¹²⁶, M. Antonelli⁵⁰, D.J.A. Antrim¹⁷, F. Anulli^{71a}, M. Aoki⁸⁰, J.A. Aparisi Pozo¹⁷⁰, M.A. Aparo¹⁵³, L. Aperio Bella⁴⁵, N. Aranzabal³⁵, V. Araujo Ferraz^{79a}, C. Arcangeletti⁵⁰, A.T.H. Arce⁴⁸, E. Arena⁸⁹, J-F. Arguin¹⁰⁷, S. Argyropoulos⁵¹, J.-H. Arling⁴⁵, A.J. Armbruster³⁵, A. Armstrong¹⁶⁷, O. Arnaez¹⁶³, H. Arnold³⁵, Z.P. Arrubarrena Tame¹¹¹, G. Artoni¹³¹, H. Asada¹¹³, K. Asai¹²³, S. Asai¹⁶⁰, N.A. Asbah⁵⁸, E.M. Asimakopoulou¹⁶⁸, L. Asquith¹⁵³, J. Assahsah^{34d}, K. Assamagan²⁸, R. Astalos^{27a}, R.J. Atkin^{32a}, M. Atkinson¹⁶⁹, N.B. Atlay¹⁸, H. Atmani^{59b}, P.A. Atmasiddha¹⁰³, K. Augsten¹³⁸, S. Auricchio^{68a,68b}, V.A. Austrup¹⁷⁸, G. Avner¹⁵⁷, G. Avolio³⁵, M.K. Ayoub^{14c}, G. Azuelos^{107,af}, D. Babal^{27a}, H. Bachacou¹⁴¹, K. Bachas¹⁵⁹, A. Bachi³³, F. Backman^{44a,44b}, A. Badea⁵⁸, P. Bagnaia^{71a,71b}, M. Bahmani¹⁸, A.J. Bailey¹⁷⁰, V.R. Bailey¹⁶⁹, J.T. Baines¹⁴⁰, C. Bakalis⁹, O.K. Baker¹⁷⁹, P.J. Bakker¹¹⁶, E. Bakos¹⁵, D. Bakshi Gupta⁷, S. Balaji¹⁵⁴, R. Balasubramanian¹¹⁶, E.M. Baldin^{118b,118a}, P. Balek¹³⁹, E. Ballabene^{67a,67b}, F. Balli¹⁴¹, L.M. Baltas^{60a}, W.K. Balunas¹³¹, J. Balz⁹⁷, E. Banas⁸³, M. Bandieramonte¹³⁵, A. Bandyopadhyay²³, S. Bansal²³, L. Barak¹⁵⁸, E.L. Barberio¹⁰², D. Barberis^{54b,54a}, M. Barbero⁹⁹, G. Barbour⁹³, K.N. Barends^{32a}, T. Barillari¹¹², M-S. Barisits³⁵, J. Barkeloo¹²⁸, T. Barklow¹⁵⁰, R.M. Barnett¹⁷, A. Baroncelli^{59a}, G. Barone²⁸, A.J. Barr¹³¹, L. Barranco Navarro^{44a,44b}, F. Barreiro⁹⁶, J. Barreiro Guimarães da Costa^{14a}, U. Barron¹⁵⁸, S. Barsov¹³⁴, F. Bartels^{60a}, R. Bartoldus¹⁵⁰, G. Bartolini⁹⁹, A.E. Barton⁸⁸, P. Bartos^{27a}, A. Basalae⁴⁵, A. Basan⁹⁷, M. Baselga⁴⁵, I. Bashta^{73a,73b}, A. Bassalat⁶³, M.J. Basso¹⁶³, C.R. Basson⁹⁸, R.L. Bates⁵⁶, S. Batlamous^{34e}, J.R. Batley³¹, B. Batool¹⁴⁸, M. Battaglia¹⁴², M. Bause^{71a,71b}, F. Bauer^{141,*}, P. Bauer²³, A. Bayirli^{11c}, J.B. Beacham⁴⁸, T. Beau¹³², P.H. Beauchemin¹⁶⁶, F. Becherer⁵¹, P. Bechtel²³, H.P. Beck^{19,p}, K. Becker¹⁷⁴, C. Becot⁴⁵, A.J. Beddall^{11c}, V.A. Bednyakov⁷⁸, C.P. Bee¹⁵², T.A. Beermann³⁵, M. Begalli^{79b}, M. Beger²⁸, A. Behera¹⁵², J.K. Behr⁴⁵, C. Beirao Da Cruz E Silva³⁵, J.F. Beirer^{52,35}, F. Beisiegel²³, M. Belfkir⁴, G. Bella¹⁵⁸, L. Bellagamba^{22b}, A. Bellerive³³, P. Bellos²⁰, K. Beloborodov^{118b,118a}, K. Belotskiy¹⁰⁹, N.L. Belyaev¹⁰⁹, D. Bencheikroun^{34a}, Y. Benhammou¹⁵⁸, D.P. Benjamin²⁸, M. Benoit²⁸, J.R. Bensinger²⁵, S. Bentvelsen¹¹⁶, L. Beresford³⁵, M. Beretta⁵⁰, D. Berge¹⁸, E. Bergeas Kuutmann¹⁶⁸, N. Berger⁴, B. Bergmann¹³⁸, L.J. Bergsten²⁵, J. Beringer¹⁷, S. Berlendis⁶, G. Bernardi¹³², C. Bernius¹⁵⁰, F.U. Bernlochner²³, T. Berry⁹², P. Berta¹³⁹, I.A. Bertram⁸⁸, O. Bessidskaia Bylund¹⁷⁸, S. Bethke¹¹², A. Betti⁴¹, A.J. Bevan⁹¹, S. Bhatta¹⁵², D.S. Bhattacharya¹⁷³, P. Bhattarai²⁵, V.S. Bhopatkar⁵, R. Bi¹³⁵, R. Bi²⁸, R.M. Bianchi¹³⁵, O. Biebel¹¹¹, R. Bielski¹²⁸, N.V. Biesuz^{70a,70b}, M. Biglietti^{73a}, T.R.V. Billoud¹³⁸, M. Bindi⁵², A. Bingul^{11d},

C. Bini^{71a,71b}, S. Biondi^{22b,22a}, A. Biondini⁸⁹, C.J. Birch-sykes⁹⁸, G.A. Bird^{20,140}, M. Birman¹⁷⁶, T. Bisanz³⁵, J.P. Biswal², D. Biswas^{177j}, A. Bitadze⁹⁸, K. Bjørke¹³⁰, I. Bloch⁴⁵, C. Blocker²⁵, A. Blue⁵⁶, U. Blumenschein⁹¹, J. Blumenthal⁹⁷, G.J. Bobbink¹¹⁶, V.S. Bobrovnikov^{118b,118a}, M. Boehler⁵¹, D. Bogavac¹³, A.G. Bogdanchikov^{118b,118a}, C. Bohm^{44a}, V. Boisvert⁹², P. Bokan⁴⁵, T. Bold^{82a}, M. Bomben¹³², M. Bona⁹¹, M. Boonekamp¹⁴¹, C.D. Booth⁹², A.G. Borbély⁵⁶, H.M. Borecka-Bielska¹⁰⁷, L.S. Borgna⁹³, G. Borissov⁸⁸, D. Bortoletto¹³¹, D. Boscherini^{22b}, M. Bosman¹³, J.D. Bossio Sola³⁵, K. Bouaouda^{34a}, J. Boudreau¹³⁵, E.V. Bouhova-Thacker⁸⁸, D. Boumediene³⁷, R. Bouquet¹³², A. Boveia¹²⁴, J. Boyd³⁵, D. Boye²⁸, I.R. Boyko⁷⁸, A.J. Bozson⁹², J. Bracinik²⁰, N. Brahim^{59d,59c}, G. Brandt¹⁷⁸, O. Brandt³¹, F. Braren⁴⁵, B. Brau¹⁰⁰, J.E. Brau¹²⁸, W.D. Breaden Madden⁵⁶, K. Brendlinger⁴⁵, R. Brenner¹⁷⁶, L. Brenner³⁵, R. Brenner¹⁶⁸, S. Bressler¹⁷⁶, B. Brickwedde⁹⁷, D. Britton⁵⁶, D. Britzger¹¹², I. Brock²³, G. Brooijmans³⁸, W.K. Brooks^{143f}, E. Brost²⁸, P.A. Bruckman de Renstrom⁸³, B. Brüers⁴⁵, D. Brunco^{27b}, A. Bruni^{22b}, G. Bruni^{22b}, M. Bruschi^{22b}, N. Brusino^{71a,71b}, L. Bryngemark¹⁵⁰, T. Buanes¹⁶, Q. Buat¹⁴⁵, P. Buchholz¹⁴⁸, A.G. Buckley⁵⁶, I.A. Budagov⁷⁸, M.K. Bugge¹³⁰, O. Bulekov¹⁰⁹, B.A. Bullard⁵⁸, S. Burdin⁸⁹, C.D. Burgard⁴⁵, A.M. Burger¹²⁶, B. Burghgrave⁷, J.T.P. Burri³¹, C.D. Burton¹⁰, J.C. Burzynski¹⁴⁹, E.L. Busch³⁸, V. Büscher⁹⁷, P.J. Bussey⁵⁶, J.M. Butler²⁴, C.M. Buttar⁵⁶, J.M. Butterworth⁹³, W. Buttinger¹⁴⁰, C.J. Buxo Vazquez¹⁰⁴, A.R. Buzykaev^{118b,118a}, G. Cabras^{22b}, S. Cabrera Urbán¹⁷⁰, D. Caforio⁵⁵, H. Cai¹³⁵, V.M.M. Cairo¹⁵⁰, O. Cakir^{3a}, N. Calace³⁵, P. Calafiura¹⁷, G. Calderini¹³², P. Calfayan⁶⁴, G. Callea⁵⁶, L.P. Caloba^{79b}, D. Calvet³⁷, S. Calvet³⁷, T.P. Calvet⁹⁹, M. Calvetti^{70a,70b}, R. Camacho Toro¹³², S. Camarda³⁵, D. Camarero Munoz⁹⁶, P. Camarri^{72a,72b}, M.T. Camerlingo^{73a,73b}, D. Cameron¹³⁰, C. Camincher¹⁷², M. Campanelli⁹³, A. Camplani³⁹, V. Canale^{68a,68b}, A. Canesse¹⁰¹, M. Cano Bret⁷⁶, J. Cantero⁹⁶, Y. Cao¹⁶⁹, F. Capocasa²⁵, M. Capua^{40b,40a}, A. Carbone^{67a,67b}, R. Cardarelli^{72a}, J.C.J. Cardenas⁷, F. Cardillo¹⁷⁰, G. Carducci^{40b,40a}, T. Carli³⁵, G. Carlino^{68a}, B.T. Carlson¹³⁵, E.M. Carlson^{172,164a}, L. Carminati^{67a,67b}, M. Carnesale^{71a,71b}, S. Caron¹¹⁵, E. Carquin^{143f}, S. Carrá⁴⁵, G. Carratta^{22b,22a}, J.W.S. Carter¹⁶³, T.M. Carter⁴⁹, D. Casadei^{32c}, M.P. Casado^{13g}, A.F. Casha¹⁶³, E.G. Castiglia¹⁷⁹, F.L. Castillo^{60a}, L. Castillo Garcia¹³, V. Castillo Gimenez¹⁷⁰, N.F. Castro^{136a,136e}, A. Catinaccio³⁵, J.R. Catmore¹³⁰, V. Cavaliere²⁸, N. Cavalli^{22b,22a}, V. Cavasinni^{70a,70b}, E. Celebi^{11c}, F. Celli¹³¹, M.S. Centonze^{66a,66b}, K. Cerny¹²⁷, A.S. Cerqueira^{79a}, A. Cerri¹⁵³, L. Cerrito^{72a,72b}, F. Cerutti¹⁷, A. Cervelli^{22b}, S.A. Cetin^{11c,z}, Z. Chadi^{34a}, D. Chakraborty¹¹⁷, M. Chala^{136f}, J. Chan¹⁷⁷, W.S. Chan¹¹⁶, W.Y. Chan⁸⁹, J.D. Chapman³¹, B. Chargeishvili^{156b}, D.G. Charlton²⁰, T.P. Charman⁹¹, M. Chatterjee¹⁹, S. Chekanov⁵, S.V. Chekulaev^{164a}, G.A. Chelkov^{78,ab}, A. Chen¹⁰³, B. Chen¹⁵⁸, B. Chen¹⁷², C. Chen^{59a}, H. Chen^{14c}, H. Chen²⁸, J. Chen^{59c}, J. Chen²⁵, S. Chen¹³³, S.J. Chen^{14c}, X. Chen^{59c}, X. Chen^{14b}, Y. Chen^{59a}, C.L. Cheng¹⁷⁷, H.C. Cheng^{61a}, A. Cheplakov⁷⁸, E. Cheremushkina⁴⁵, E. Cherepanova⁷⁸, R. Cherkaoui El Moursli^{34e}, E. Cheu⁶, K. Cheung⁶², L. Chevalier¹⁴¹, V. Chiarella⁵⁰, G. Chiarelli^{70a}, G. Chiodini^{66a}, A.S. Chisholm²⁰, A. Chitan^{26b}, Y.H. Chiu¹⁷², M.V. Chizhov⁷⁸, K. Choi¹⁰, A.R. Chomont^{71a,71b}, Y. Chou¹⁰⁰, Y.S. Chow¹¹⁶, T. Chowdhury^{32g}, L.D. Christopher^{32g}, M.C. Chu^{61a}, X. Chu^{14a,14d}, J. Chudoba¹³⁷, J.J. Chwastowski⁸³, D. Cieri¹¹², K.M. Ciesla⁸³, V. Cindro⁹⁰, I.A. Cioară^{26b}, A. Ciocio¹⁷, F. Ciroto^{68a,68b}, Z.H. Citron^{176,k}, M. Citterio^{67a}, D.A. Ciubotaru^{26b}, B.M. Ciungu¹⁶³, A. Clark⁵³, P.J. Clark⁴⁹, J.M. Clavijo Columbie⁴⁵, S.E. Clawson⁹⁸, C. Clement^{44a,44b}, L. Clissa^{22b,22a}, Y. Coadou⁹⁹, M. Cobal^{165a,65c}, A. Coccaro^{54b}, R.F. Coelho Barrue^{136a}, R. Coelho Lopes De Sa¹⁰⁰, S. Coelli^{67a}, H. Cohen¹⁵⁸, A.E.C. Coimbra³⁵, B. Cole³⁸, J. Collot⁵⁷, P. Conde Muiño^{136a,136g}, S.H. Connell^{32c}, I.A. Connelly⁵⁶, E.I. Conroy¹³¹, F. Conventi^{68a,ag}, H.G. Cooke²⁰, A.M. Cooper-Sarkar¹³¹, F. Cormier¹⁷¹, L.D. Corpe³⁵, M. Corradi^{71a,71b}, E.E. Corrigan⁹⁵, F. Corriveau^{101,v}, M.J. Costa¹⁷⁰, F. Costanza⁴, D. Costanzo¹⁴⁶, B.M. Cote¹²⁴, G. Cowan⁹², J.W. Cowley³¹, K. Cranmer¹²², S. Crépe-Renaudin⁵⁷, F. Crescioli¹³², M. Cristinziani¹⁴⁸, M. Cristoforetti^{74a,74b,b}, V. Croft¹⁶⁶, G. Crosetti^{40b,40a}, A. Cueto³⁵, T. Cuhadar Donszelmann¹⁶⁷, H. Cui^{14a,14d}, Z. Cui⁶, A.R. Cukierman¹⁵⁰, W.R. Cunningham⁵⁶, F. Curcio^{40b,40a}, P. Czodrowski³⁵, M.M. Czurylo^{60b},

M.J. Da Cunha Sargedas De Sousa^{59a}, J.V. Da Fonseca Pinto^{79b}, C. Da Via⁹⁸, W. Dabrowski^{82a}, T. Dado⁴⁶,
S. Dahbi^{32g}, T. Dai¹⁰³, C. Dallapiccola¹⁰⁰, M. Dam³⁹, G. D'amen²⁸, V. D'Amico^{73a,73b}, J. Damp⁹⁷,
J.R. Dandoy¹³³, M.F. Daneri²⁹, M. Danninger¹⁴⁹, V. Dao³⁵, G. Darbo^{54b}, S. Darmora⁵, A. Dattagupta¹²⁸,
S. D'Auria^{67a,67b}, C. David^{164b}, T. Davidek¹³⁹, D.R. Davis⁴⁸, B. Davis-Purcell³³, I. Dawson⁹¹, K. De⁷,
R. De Asmundis^{68a}, M. De Beurs¹¹⁶, S. De Castro^{22b,22a}, N. De Groot¹¹⁵, P. de Jong¹¹⁶, H. De la Torre¹⁰⁴,
A. De Maria^{14c}, A. De Salvo^{71a}, U. De Sanctis^{72a,72b}, M. De Santis^{72a,72b}, A. De Santo¹⁵³,
J.B. De Vivie De Regie⁵⁷, D.V. Dedovich⁷⁸, J. Degens¹¹⁶, A.M. Deiana⁴¹, J. Del Peso⁹⁶, F. Del Rio^{60a},
F. Deliot¹⁴¹, C.M. Delitzsch⁶, M. Della Pietra^{68a,68b}, D. Della Volpe⁵³, A. Dell'Acqua³⁵,
L. Dell'Asta^{67a,67b}, M. Delmastro⁴, P.A. Delsart⁵⁷, S. Demers¹⁷⁹, M. Demichev⁷⁸, S.P. Denisov¹¹⁹,
L. D'Eramo¹¹⁷, D. Derendarz⁸³, F. Derue¹³², P. Dervan⁸⁹, K. Desch²³, K. Dette¹⁶³, C. Deutsch²³,
P.O. Deviveiros³⁵, F.A. Di Bello^{71a,71b}, A. Di Ciaccio^{72a,72b}, L. Di Ciaccio⁴, A. Di Domenico^{71a,71b},
C. Di Donato^{68a,68b}, A. Di Girolamo³⁵, G. Di Gregorio^{70a,70b}, A. Di Luca^{74a,74b,b}, B. Di Micco^{73a,73b},
R. Di Nardo^{73a,73b}, C. Diaconu⁹⁹, F.A. Dias¹¹⁶, T. Dias Do Vale^{136a}, M.A. Diaz^{143a}, F.G. Diaz Capriles²³,
M. Didenko¹⁷⁰, E.B. Diehl¹⁰³, S. Díez Cornell⁴⁵, C. Diez Pardos¹⁴⁸, C. Dimitriadi^{23,168}, A. Dimitrievska¹⁷,
W. Ding^{14b}, J. Dingfelder²³, I.M. Dinu^{26b}, S.J. Dittmeier^{60b}, F. Dittus³⁵, F. Djama⁹⁹, T. Djobava^{156b},
J.I. Djuvsland¹⁶, M.A.B. Do Vale¹⁴⁴, D. Dodsworth²⁵, C. Doglioni⁹⁵, J. Dolejsi¹³⁹, Z. Dolezal¹³⁹,
M. Donadelli^{79c}, B. Dong^{59c}, J. Donini³⁷, A. D'onofrio^{14c}, M. D'Onofrio⁸⁹, J. Dopke¹⁴⁰, A. Doria^{68a},
M.T. Dova⁸⁷, A.T. Doyle⁵⁶, E. Drechsler¹⁴⁹, E. Dreyer¹⁷⁶, A.S. Drobac¹⁶⁶, D. Du^{59a}, T.A. du Pree¹¹⁶,
F. Dubinin¹⁰⁸, M. Dubovsky^{27a}, E. Duchovni¹⁷⁶, G. Duckeck¹¹¹, O.A. Ducu^{35,26b}, D. Duda¹¹²,
A. Dudarev³⁵, M. D'uffizi⁹⁸, L. Duflot⁶³, M. Dührssen³⁵, C. Dülsen¹⁷⁸, A.E. Dumitriu^{26b}, M. Dunford^{60a},
S. Dungs⁴⁶, K. Dunne^{44a,44b}, A. Duperrin⁹⁹, H. Duran Yildiz^{3a}, M. Düren⁵⁵, A. Durglishvili^{156b},
B. Dutta⁴⁵, G.I. Dyckes¹⁷, M. Dyndal^{82a}, S. Dysch⁹⁸, B.S. Dziedzic⁸³, B. Eckerova^{27a}, M.G. Eggleston⁴⁸,
E. Egidio Purcino De Souza^{79b}, L.F. Ehrke⁵³, G. Eigen¹⁶, K. Einsweiler¹⁷, T. Ekelof¹⁶⁸, Y. El Ghazali^{34b},
H. El Jarrari^{34e}, A. El Moussaouy^{34a}, V. Ellajosyula¹⁶⁸, M. Ellert¹⁶⁸, F. Ellinghaus¹⁷⁸, A.A. Elliot⁹¹,
N. Ellis³⁵, J. Elmsheuser²⁸, M. Elsing³⁵, D. Emeliyanov¹⁴⁰, A. Emerman³⁸, Y. Enari¹⁶⁰, J. Erdmann⁴⁶,
A. Ereditato¹⁹, P.A. Erland⁸³, M. Errenst¹⁷⁸, M. Escalier⁶³, C. Escobar¹⁷⁰, O. Estrada Pastor¹⁷⁰,
E. Etzion¹⁵⁸, G. Evans^{136a}, H. Evans⁶⁴, M.O. Evans¹⁵³, A. Ezhilov¹³⁴, S. Ezzarqtouni^{34a}, F. Fabbri⁵⁶,
L. Fabbri^{22b,22a}, G. Facini¹⁷⁴, V. Fadeyev¹⁴², R.M. Fakhruddinov¹¹⁹, S. Falciano^{71a}, P.J. Falke²³, S. Falke³⁵,
J. Faltova¹³⁹, Y. Fan^{14a}, Y. Fang^{14a}, G. Fanourakis⁴³, M. Fanti^{67a,67b}, M. Faraj^{59c}, A. Farbin⁷, A. Farilla^{73a},
E.M. Farina^{69a,69b}, T. Farooque¹⁰⁴, S.M. Farrington⁴⁹, F. Fassi^{34e}, D. Fassouliotis⁸,
M. Faucci Giannelli^{72a,72b}, W.J. Fawcett³¹, L. Fayard⁶³, O.L. Fedin^{134,o}, G. Fedotov¹³⁴, M. Feickert¹⁶⁹,
L. Feligioni⁹⁹, A. Fell¹⁴⁶, C. Feng^{59b}, M. Feng^{14b}, M.J. Fenton¹⁶⁷, A.B. Fenyuk¹¹⁹, S.W. Ferguson⁴²,
J.A. Fernandez Pretel⁵¹, J. Ferrando⁴⁵, A. Ferrari¹⁶⁸, P. Ferrari¹¹⁶, R. Ferrari^{69a}, D. Ferrere⁵³,
C. Ferretti¹⁰³, F. Fiedler⁹⁷, A. Filipčič⁹⁰, F. Filthaut¹¹⁵, M.C.N. Fiolhais^{136a,136c,a}, L. Fiorini¹⁷⁰,
F. Fischer¹⁴⁸, W.C. Fisher¹⁰⁴, T. Fitschen²⁰, I. Fleck¹⁴⁸, P. Fleischmann¹⁰³, T. Flick¹⁷⁸, L. Flores¹³³,
M. Flores^{32d}, L.R. Flores Castillo^{61a}, F.M. Follega^{74a,74b}, N. Fomin¹⁶, J.H. Foo¹⁶³, B.C. Forland⁶⁴,
A. Formica¹⁴¹, F.A. Förster¹³, A.C. Forti⁹⁸, E. Fortin⁹⁹, M.G. Foti¹³¹, L. Fountas⁸, D. Fournier⁶³,
H. Fox⁸⁸, P. Francavilla^{70a,70b}, S. Francescato⁵⁸, M. Franchini^{22b,22a}, S. Franchino^{60a}, D. Francis³⁵,
L. Franco⁴, L. Franconi¹⁹, M. Franklin⁵⁸, G. Frattari^{71a,71b}, A.C. Freegard⁹¹, P.M. Freeman²⁰,
W.S. Freund^{79b}, E.M. Freundlich⁴⁶, D. Froidevaux³⁵, J.A. Frost¹³¹, Y. Fu^{59a}, M. Fujimoto¹²³,
E. Fullana Torregrosa¹⁷⁰, J. Fuster¹⁷⁰, A. Gabrielli^{22b,22a}, A. Gabrielli³⁵, P. Gadow⁴⁵, G. Gagliardi^{54b,54a},
L.G. Gagnon¹⁷, G.E. Gallardo¹³¹, E.J. Gallas¹³¹, B.J. Gallop¹⁴⁰, R. Gamboa Goni⁹¹, K.K. Gan¹²⁴,
S. Ganguly¹⁶⁰, J. Gao^{59a}, Y. Gao⁴⁹, F.M. Garay Walls^{143a}, C. García¹⁷⁰, J.E. García Navarro¹⁷⁰,
J.A. García Pascual^{14a}, M. Garcia-Sciveres¹⁷, R.W. Gardner³⁶, D. Garg⁷⁶, R.B. Garg¹⁵⁰, S. Gargiulo⁵¹,
C.A. Garner¹⁶³, V. Garonne²⁸, S.J. Gasiorowski¹⁴⁵, P. Gaspar^{79b}, G. Gaudio^{69a}, P. Gauzzi^{71a,71b},
I.L. Gavrilenko¹⁰⁸, A. Gavriluk¹²⁰, C. Gay¹⁷¹, G. Gaycken⁴⁵, E.N. Gazis⁹, A.A. Geanta^{26b}, C.M. Gee¹⁴²,
J. Geisen⁹⁵, M. Geisen⁹⁷, C. Gemme^{54b}, M.H. Genest⁵⁷, S. Gentile^{71a,71b}, S. George⁹², W.F. George²⁰,

T. Geralis⁴³, L.O. Gerlach⁵², P. Gessinger-Befurt³⁵, M. Ghasemi Bostanabad¹⁷², A. Ghosh¹⁶⁷, A. Ghosh⁶, B. Giacobbe^{22b}, S. Giagu^{71a,71b}, N. Giangiacomi¹⁶³, P. Giannetti^{70a}, A. Giannini^{68a,68b}, S.M. Gibson⁹², M. Gignac¹⁴², D.T. Gil^{82b}, B.J. Gilbert³⁸, D. Gillberg³³, G. Gilles¹¹⁶, N.E.K. Gillwald⁴⁵, D.M. Gingrich^{2,af}, M.P. Giordani^{65a,65c}, P.F. Giraud¹⁴¹, G. Giugliarelli^{65a,65c}, D. Giugni^{67a}, F. Giuli^{72a,72b}, I. Gkialas^{8,h}, P. Gkoutoumis⁹, L.K. Gladilin¹¹⁰, C. Glasman⁹⁶, G.R. Gledhill¹²⁸, M. Glisic¹²⁸, I. Gnesi^{40b,d}, Y. Go²⁸, M. Goblirsch-Kolb²⁵, D. Godin¹⁰⁷, S. Goldfarb¹⁰², T. Golling⁵³, D. Golubkov¹¹⁹, J.P. Gombas¹⁰⁴, A. Gomes^{136a,136b}, R. Goncalves Gama⁵², R. Gonçalo^{136a,136c}, G. Gonella¹²⁸, L. Gonella²⁰, A. Gongadze⁷⁸, F. Gonnella²⁰, J.L. Gonski³⁸, S. González de la Hoz¹⁷⁰, S. Gonzalez Fernandez¹³, R. Gonzalez Lopez⁸⁹, C. Gonzalez Renteria¹⁷, R. Gonzalez Suarez¹⁶⁸, S. Gonzalez-Sevilla⁵³, G.R. Gonzalvo Rodriguez¹⁷⁰, R.Y. González Andana⁴⁹, L. Goossens³⁵, N.A. Gorasia²⁰, P.A. Gorbounov¹²⁰, H.A. Gordon²⁸, B. Gorini³⁵, E. Gorini^{66a,66b}, A. Gorišek⁹⁰, A.T. Goshaw⁴⁸, M.I. Gostkin⁷⁸, C.A. Gottardo¹¹⁵, M. Gouighri^{34b}, V. Goumarre⁴⁵, A.G. Goussiou¹⁴⁵, N. Govender^{32c}, C. Goy⁴, I. Grabowska-Bold^{182a}, K. Graham³³, E. Gramstad¹³⁰, S. Grancagnolo¹⁸, M. Grandi¹⁵³, V. Gratchev¹³⁴, P.M. Gravila^{26f}, F.G. Gravili^{66a,66b}, H.M. Gray¹⁷, C. Greife²³, I.M. Gregor⁴⁵, P. Grenier¹⁵⁰, K. Grevtsov⁴⁵, C. Grieco¹³, N.A. Grieser¹²⁵, A.A. Grillo¹⁴², K. Grimm^{30,1}, S. Grinstein^{13,t}, J.-F. Grivaz⁶³, S. Groh⁹⁷, E. Gross¹⁷⁶, J. Grosse-Knetter⁵², C. Grud¹⁰³, A. Grummer¹¹⁴, J.C. Grundy¹³¹, L. Guan¹⁰³, W. Guan¹⁷⁷, C. Gubbels¹⁷¹, J.G.R. Guerrero Rojas¹⁷⁰, F. Guescini¹¹², D. Guest¹⁸, R. Gugel⁹⁷, A. Guida⁴⁵, T. Guillemin⁴, S. Guindon³⁵, F. Guo^{14a}, J. Guo^{59c}, L. Guo⁶³, Y. Guo¹⁰³, R. Gupta⁴⁵, S. Gurbuz²³, G. Gustavino³⁵, M. Guth⁵³, P. Gutierrez¹²⁵, L.F. Gutierrez Zagazeta¹³³, C. Gutschow⁹³, C. Guyot¹⁴¹, C. Gwenlan¹³¹, C.B. Gwilliam⁸⁹, E.S. Haaland¹³⁰, A. Haas¹²², M. Habedank⁴⁵, C. Haber¹⁷, H.K. Hadavand⁷, A. Hadef⁹⁷, S. Hadzic¹¹², M. Haleem¹⁷³, J. Haley¹²⁶, J.J. Hall¹⁴⁶, G.D. Hallewell⁹⁹, L. Halser¹⁹, K. Hamano¹⁷², H. Hamdaoui^{34e}, M. Hamer²³, G.N. Hamity⁴⁹, K. Han^{59a}, L. Han^{14c}, L. Han^{59a}, S. Han¹⁷, Y.F. Han¹⁶³, K. Hanagaki^{80,r}, M. Hance¹⁴², D.A. Hangal³⁸, M.D. Hank³⁶, R. Hankache⁹⁸, E. Hansen⁹⁵, J.B. Hansen³⁹, J.D. Hansen³⁹, P.H. Hansen³⁹, K. Hara¹⁶⁵, T. Harenberg¹⁷⁸, S. Harkusha¹⁰⁵, Y.T. Harris¹³¹, P.F. Harrison¹⁷⁴, N.M. Hartman¹⁵⁰, N.M. Hartmann¹¹¹, Y. Hasegawa¹⁴⁷, A. Hasib⁴⁹, S. Haug¹⁹, R. Hauser¹⁰⁴, M. Havranek¹³⁸, C.M. Hawkes²⁰, R.J. Hawkings³⁵, S. Hayashida¹¹³, D. Hayden¹⁰⁴, C. Hayes¹⁰³, R.L. Hayes¹⁷¹, C.P. Hays¹³¹, J.M. Hays⁹¹, H.S. Hayward⁸⁹, F. He^{59a}, Y. He¹⁶¹, Y. He¹³², M.P. Heath⁴⁹, V. Hedberg⁹⁵, A.L. Heggelund¹³⁰, N.D. Hehir⁹¹, C. Heidegger⁵¹, K.K. Heidegger⁵¹, W.D. Heidorn⁷⁷, J. Heilman³³, S. Heim⁴⁵, T. Heim¹⁷, B. Heinemann^{45,ad}, J.G. Heinlein¹³³, J.J. Heinrich¹²⁸, L. Heinrich³⁵, J. Hejbal¹³⁷, L. Helary⁴⁵, A. Held¹²², C.M. Helling¹⁴², S. Hellman^{44a,44b}, C. Hensens³⁵, R.C.W. Henderson⁸⁸, L. Henkelmann³¹, A.M. Henriques Correia³⁵, H. Herde¹⁵⁰, Y. Hernández Jiménez¹⁵², H. Herr⁹⁷, M.G. Herrmann¹¹¹, T. Herrmann⁴⁷, G. Herten⁵¹, R. Hertenberger¹¹¹, L. Hervas³⁵, N.P. Hessey^{164a}, H. Hibi⁸¹, S. Higashino⁸⁰, E. Higón-Rodríguez¹⁷⁰, S.J. Hillier²⁰, I. Hinchliffe¹⁷, F. Hinterkeuser²³, M. Hirose¹²⁹, S. Hirose¹⁶⁵, D. Hirschbuehl¹⁷⁸, B. Hiti⁹⁰, O. Hladik¹³⁷, J. Hobbs¹⁵², R. Hobincu^{26e}, N. Hod¹⁷⁶, M.C. Hodgkinson¹⁴⁶, B.H. Hodgkinson³¹, A. Hoecker³⁵, J. Hofer⁴⁵, D. Hohn⁵¹, T. Holm²³, M. Holzbock¹¹², L.B.A.H. Hommels³¹, B.P. Honan⁹⁸, J. Hong^{59c}, T.M. Hong¹³⁵, Y. Hong⁵², J.C. Honig⁵¹, A. Hönle¹¹², B.H. Hooberman¹⁶⁹, W.H. Hopkins⁵, Y. Horii¹¹³, L.A. Horyn³⁶, S. Hou¹⁵⁵, J. Howarth⁵⁶, J. Hoya⁸⁷, M. Hrabovsky¹²⁷, A. Hrynevich¹⁰⁶, T. Hryn'ova⁴, P.J. Hsu⁶², S.-C. Hsu¹⁴⁵, Q. Hu³⁸, S. Hu^{59c}, Y.F. Hu^{14a,14d,ah}, D.P. Huang⁹³, X. Huang^{14c}, Y. Huang^{59a}, Y. Huang^{14a}, Z. Hubacek¹³⁸, M. Huebner²³, F. Huegging²³, T.B. Huffman¹³¹, M. Huhtinen³⁵, S.K. Huiberts¹⁶, R. Hulsken⁵⁷, N. Huseynov^{12,aa}, J. Huston¹⁰⁴, J. Huth⁵⁸, R. Hyneman¹⁵⁰, S. Hyrych^{27a}, G. Iacobucci⁵³, G. Iakovidis²⁸, I. Ibragimov¹⁴⁸, L. Iconomidou-Fayard⁶³, P. Iengo³⁵, R. Iguchi¹⁶⁰, T. Iizawa⁵³, Y. Ikegami⁸⁰, A. Ilg¹⁹, N. Ilic¹⁶³, H. Imam^{34a}, T. Ingebretsen Carlson^{44a,44b}, G. Introzzi^{69a,69b}, M. Iodice^{73a}, V. Ippolito^{71a,71b}, M. Ishino¹⁶⁰, W. Islam¹⁷⁷, C. Issever^{18,45}, S. Istin^{11c,ai}, H. Ito¹⁷⁵, J.M. Iturbe Ponce^{61a}, R. Iuppa^{74a,74b}, A. Ivina¹⁷⁶, J.M. Izen⁴², V. Izzo^{68a}, P. Jacka¹³⁷, P. Jackson¹, R.M. Jacobs⁴⁵, B.P. Jaeger¹⁴⁹, C.S. Jagfeld¹¹¹, G. Jäkel¹⁷⁸, K. Jakobs⁵¹, T. Jakoubek¹⁷⁶, J. Jamieson⁵⁶, K.W. Janas^{82a}, G. Jarlskog⁹⁵, A.E. Jaspan⁸⁹, T. Javůrek³⁵, M. Javurkova¹⁰⁰, F. Jeanneau¹⁴¹, L. Jeanty¹²⁸,

J. Jejelava^{156a,w}, P. Jenni^{51,e}, S. Jézéquel⁴, J. Jia¹⁵², Z. Jia^{14c}, Y. Jiang^{59a}, S. Jiggins⁴⁹, J. Jimenez Pena¹¹², S. Jin^{14c}, A. Jinaru^{26b}, O. Jinnouchi¹⁶¹, H. Jivan^{32g}, P. Johansson¹⁴⁶, K.A. Johns⁶, C.A. Johnson⁶⁴, D.M. Jones³¹, E. Jones¹⁷⁴, R.W.L. Jones⁸⁸, T.J. Jones⁸⁹, J. Jovicevic¹⁵, X. Ju¹⁷, J.J. Junggeburth³⁵, A. Juste Rozas^{13,t}, S. Kabana^{143e}, A. Kaczmarska⁸³, M. Kado^{71a,71b}, H. Kagan¹²⁴, M. Kagan¹⁵⁰, A. Kahn³⁸, A. Kahn¹³³, C. Kahra⁹⁷, T. Kaji¹⁷⁵, E. Kajomovitz¹⁵⁷, C.W. Kalderon²⁸, A. Kamenshchikov¹¹⁹, N.J. Kang¹⁴², Y. Kano¹¹³, D. Kar^{32g}, K. Karava¹³¹, M.J. Kareem^{164b}, E. Karentzos⁵¹, I. Karkanias¹⁵⁹, S.N. Karpov⁷⁸, Z.M. Karpova⁷⁸, V. Kartvelishvili⁸⁸, A.N. Karyukhin¹¹⁹, E. Kasimi¹⁵⁹, C. Kato^{59d}, J. Katzy⁴⁵, S. Kaur³³, K. Kawade¹⁴⁷, K. Kawagoe⁸⁶, T. Kawaguchi¹¹³, T. Kawamoto¹⁴¹, G. Kawamura⁵², E.F. Kay¹⁷², F.I. Kaya¹⁶⁶, S. Kazakos¹³, V.F. Kazanin^{118b,118a}, Y. Ke¹⁵², J.M. Keaveney^{32a}, R. Keeler¹⁷², J.S. Keller³³, A.S. Kelly⁹³, D. Kelsey¹⁵³, J.J. Kempster²⁰, J. Kendrick²⁰, K.E. Kennedy³⁸, O. Kepka¹³⁷, S. Kersten¹⁷⁸, B.P. Kerševan⁹⁰, S. Ketabchi Haghighat¹⁶³, M. Khandoga¹³², A. Khanov¹²⁶, A.G. Kharlamov^{118b,118a}, T. Kharlamova^{118b,118a}, E.E. Khoda¹⁴⁵, T.J. Khoo¹⁸, G. Khoraiuli¹⁷³, E. Khramov⁷⁸, J. Khubua^{156b}, M. Kiehn³⁵, A. Kilgallon¹²⁸, E. Kim¹⁶¹, Y.K. Kim³⁶, N. Kimura⁹³, A. Kirchhoff⁵², D. Kirchmeier⁴⁷, C. Kirfel²³, J. Kirk¹⁴⁰, A.E. Kiryunin¹¹², T. Kishimoto¹⁶⁰, D.P. Kisliuk¹⁶³, C. Kitsaki⁹, O. Kivernyk²³, M. Klassen^{60a}, C. Klein³³, L. Klein¹⁷³, M.H. Klein¹⁰³, M. Klein⁸⁹, U. Klein⁸⁹, P. Klimek³⁵, A. Klimentov²⁸, F. Klimpel¹¹², T. Klingl²³, T. Klioutchnikova³⁵, F.F. Klitzner¹¹¹, P. Kluit¹¹⁶, S. Kluth¹¹², E. Kneringer⁷⁵, T.M. Knight¹⁶³, A. Knue⁵¹, D. Kobayashi⁸⁶, R. Kobayashi⁸⁴, M. Kocian¹⁵⁰, T. Kodama¹⁶⁰, P. Kodys¹³⁹, D.M. Koeck¹⁵³, P.T. Koenig²³, T. Koffas³³, N.M. Köhler³⁵, M. Kolb¹⁴¹, I. Koletsou⁴, T. Komarek¹²⁷, K. Köneke⁵¹, A.X.Y. Kong¹, T. Kono¹²³, V. Konstantinides⁹³, N. Konstantinidis⁹³, B. Konya⁹⁵, R. Kopeliansky⁶⁴, S. Koperny^{82a}, K. Korcyl⁸³, K. Kordas¹⁵⁹, G. Koren¹⁵⁸, A. Korn⁹³, S. Korn⁵², I. Korolkov¹³, N. Korotkova¹¹⁰, B. Kortman¹¹⁶, O. Kortner¹¹², S. Kortner¹¹², W.H. Kostecka¹¹⁷, V.V. Kostyukhin^{148,162}, A. Kotsokechagia⁶³, A. Kotwal⁴⁸, A. Koulouris³⁵, A. Kourkoumeli-Charalampidi^{69a,69b}, C. Kourkoumelis⁸, E. Kourlitis⁵, O. Kovanda¹⁵³, R. Kowalewski¹⁷², W. Kozanecki¹⁴¹, A.S. Kozhin¹¹⁹, V.A. Kramarenko¹¹⁰, G. Kramberger⁹⁰, P. Kramer⁹⁷, D. Krasnopevtsev^{59a}, M.W. Krasny¹³², A. Krasznahorkay³⁵, J.A. Kremer⁹⁷, J. Kretzschmar⁸⁹, K. Kreul¹⁸, P. Krieger¹⁶³, F. Krieter¹¹¹, S. Krishnamurthy¹⁰⁰, A. Krishnan^{60b}, M. Krivos¹³⁹, K. Krizka¹⁷, K. Kroeninger⁴⁶, H. Kroha¹¹², J. Kroll¹³⁷, J. Kroll¹³³, K.S. Krowpman¹⁰⁴, U. Kruchonak⁷⁸, H. Krüger²³, N. Krumnack⁷⁷, M.C. Kruse⁴⁸, J.A. Krzysiak⁸³, A. Kubota¹⁶¹, O. Kuchinskaia¹⁶², S. Kuday^{3a}, D. Kuechler⁴⁵, J.T. Kuechler⁴⁵, S. Kuehn³⁵, T. Kuhl⁴⁵, V. Kukhtin⁷⁸, Y. Kulchitsky^{105,aa}, S. Kuleshov^{143d}, M. Kumar^{32g}, N. Kumari⁹⁹, M. Kuna⁵⁷, A. Kupco¹³⁷, T. Kupfer⁴⁶, O. Kuprash⁵¹, H. Kurashige⁸¹, L.L. Kurchaninov^{164a}, Y.A. Kurochkin¹⁰⁵, A. Kurova¹⁰⁹, E.S. Kuwertz³⁵, M. Kuze¹⁶¹, A.K. Kvam¹⁴⁵, J. Kvita¹²⁷, T. Kwan¹⁰¹, K.W. Kwok^{61a}, C. Lacasta¹⁷⁰, F. Lacava^{71a,71b}, H. Lacker¹⁸, D. Lacour¹³², N.N. Lad⁹³, E. Ladygin⁷⁸, B. Laforge¹³², T. Lagouri^{143e}, S. Lai⁵², I.K. Lakomic^{82a}, N. Lalloue⁵⁷, J.E. Lambert¹²⁵, S. Lammers⁶⁴, W. Lampl⁶, C. Lampoudis¹⁵⁹, E. Lançon²⁸, U. Landgraf⁵¹, M.P.J. Landon⁹¹, V.S. Lang⁵¹, J.C. Lange⁵², R.J. Langenberg¹⁰⁰, A.J. Lankford¹⁶⁷, F. Lanni²⁸, K. Lantzs²³, A. Lanza^{69a}, A. Lapertosa^{54b,54a}, J.F. Laporte¹⁴¹, T. Lari^{67a}, F. Lasagni Manghi^{22b}, M. Lassnig³⁵, V. Latonova¹³⁷, T.S. Lau^{61a}, A. Laudrain⁹⁷, A. Laurier³³, M. Lavorgna^{68a,68b}, S.D. Lawlor⁹², Z. Lawrence⁹⁸, M. Lazzaroni^{67a,67b}, B. Le⁹⁸, B. Leban⁹⁰, A. Lebedev⁷⁷, M. LeBlanc³⁵, T. LeCompte⁵, F. Ledroit-Guillon⁵⁷, A.C.A. Lee⁹³, G.R. Lee¹⁶, L. Lee⁵⁸, S.C. Lee¹⁵⁵, L.L. Leeuw^{32c}, B. Lefebvre^{164a}, H.P. Lefebvre⁹², M. Lefebvre¹⁷², C. Leggett¹⁷, K. Lehmann¹⁴⁹, G. Lehmann Miotto³⁵, W.A. Leight⁴⁵, A. Leisos^{159,s}, M.A.L. Leite^{79c}, C.E. Leitgeb⁴⁵, R. Leitner¹³⁹, K.J.C. Leney⁴¹, T. Lenz²³, S. Leone^{70a}, C. Leonidopoulos⁴⁹, A. Leopold¹⁵¹, C. Leroy¹⁰⁷, R. Les¹⁰⁴, C.G. Lester³¹, M. Levchenko¹³⁴, J. Levêque⁴, D. Levin¹⁰³, L.J. Levinson¹⁷⁶, D.J. Lewis²⁰, B. Li^{14b}, B. Li^{59b}, C. Li^{59a}, C-Q. Li^{59c,59d}, H. Li^{59a}, H. Li^{59b}, H. Li^{59b}, J. Li^{59c}, K. Li¹⁴⁵, L. Li^{59c}, M. Li^{14a,14d}, Q.Y. Li^{59a}, S. Li^{59d,59c,c}, T. Li^{59b}, X. Li⁴⁵, Z. Li^{59b}, Z. Li¹³¹, Z. Li¹⁰¹, Z. Li⁸⁹, Z. Liang^{14a}, M. Liberatore⁴⁵, B. Liberti^{72a}, K. Lie^{61c}, J. Lieber Marin^{79b}, K. Lin¹⁰⁴, R.A. Linck⁶⁴, R.E. Lindley⁶, J.H. Lindon², A. Linss⁴⁵, E. Lipeles¹³³, A. Lipniacka¹⁶, T.M. Liss^{169,ae}, A. Lister¹⁷¹, J.D. Little⁷, B. Liu^{14a}, B.X. Liu¹⁴⁹, D. Liu^{59d,59c}, J.B. Liu^{59a}, J.K.K. Liu³⁶,

K. Liu^{59d,59c}, M. Liu^{59a}, M.Y. Liu^{59a}, P. Liu^{14a}, Q. Liu^{59d,145,59c}, X. Liu^{59a}, Y. Liu⁴⁵, Y. Liu^{14c,14d},
 Y.L. Liu¹⁰³, Y.W. Liu^{59a}, M. Livan^{69a,69b}, J. Llorente Merino¹⁴⁹, S.L. Lloyd⁹¹, E.M. Lobodzinska⁴⁵,
 P. Loch⁶, S. Loffredo^{72a,72b}, T. Lohse¹⁸, K. Lohwasser¹⁴⁶, M. Lokajicek¹³⁷, J.D. Long¹⁶⁹,
 I. Longarini^{71a,71b}, L. Longo³⁵, R. Longo¹⁶⁹, I. Lopez Paz³⁵, A. Lopez Solis⁴⁵, J. Lorenz¹¹¹,
 N. Lorenzo Martinez⁴, A.M. Lory¹¹¹, A. Lösle⁵¹, X. Lou^{44a,44b}, X. Lou^{14a}, A. Lounis⁶³, J. Love⁵,
 P.A. Love⁸⁸, J.J. Lozano Bahilo¹⁷⁰, G. Lu^{14a}, M. Lu^{59a}, S. Lu¹³³, Y.J. Lu⁶², H.J. Lubatti¹⁴⁵, C. Luci^{71a,71b},
 F.L. Lucio Alves^{14c}, A. Lucotte⁵⁷, F. Luehring⁶⁴, I. Luise¹⁵², O. Lundberg¹⁵¹, B. Lund-Jensen¹⁵¹,
 N.A. Luongo¹²⁸, M.S. Lutz¹⁵⁸, D. Lynn²⁸, H. Lyons⁸⁹, R. Lysak¹³⁷, E. Lytken⁹⁵, F. Lyu^{14a},
 V. Lyubushkin⁷⁸, T. Lyubushkina⁷⁸, H. Ma²⁸, L.L. Ma^{59b}, Y. Ma⁹³, D.M. Mac Donell¹⁷², G. Maccarrone⁵⁰,
 C.M. Macdonald¹⁴⁶, J.C. MacDonald¹⁴⁶, R. Madar³⁷, W.F. Mader⁴⁷, J. Maeda⁸¹, T. Maeno²⁸,
 M. Maerker⁴⁷, V. Magerl⁵¹, J. Magro^{65a,65c}, D.J. Mahon³⁸, C. Maidantchik^{79b}, A. Maio^{136a,136b,136d},
 K. Maj^{82a}, O. Majersky^{27a}, S. Majewski¹²⁸, N. Makovec⁶³, V. Maksimovic¹⁵, B. Malaescu¹³²,
 Pa. Malecki⁸³, V.P. Maleev¹³⁴, F. Malek⁵⁷, D. Malito^{40b,40a}, U. Mallik⁷⁶, C. Malone³¹, S. Maltezos⁹,
 S. Malyukov⁷⁸, J. Mamuzic¹⁷⁰, G. Mancini⁵⁰, J.P. Mandalia⁹¹, I. Mandić⁹⁰,
 L. Manhaes de Andrade Filho^{79a}, I.M. Maniatis¹⁵⁹, M. Manisha¹⁴¹, J. Manjarres Ramos⁴⁷,
 D.C. Mankad¹⁷⁶, K.H. Mankinen⁹⁵, A. Mann¹¹¹, A. Manousos⁷⁵, B. Mansoulie¹⁴¹, S. Manzoni³⁵,
 A. Marantis^{159,s}, G. Marchiori¹³², M. Marcisovsky¹³⁷, L. Marcocchia^{72a,72b}, C. Marcon⁹⁵,
 M. Marjanovic¹²⁵, Z. Marshall¹⁷, S. Marti-Garcia¹⁷⁰, T.A. Martin¹⁷⁴, V.J. Martin⁴⁹, B. Martin dit Latour¹⁶,
 L. Martinelli^{71a,71b}, M. Martinez^{13,t}, P. Martinez Agullo¹⁷⁰, V.I. Martinez Outschoorn¹⁰⁰,
 S. Martin-Haugh¹⁴⁰, V.S. Martoiu^{26b}, A.C. Martyniuk⁹³, A. Marzin³⁵, S.R. Maschek¹¹², L. Masetti⁹⁷,
 T. Mashimo¹⁶⁰, J. Masik⁹⁸, A.L. Maslennikov^{118b,118a}, L. Massa^{22b}, P. Massarotti^{68a,68b},
 P. Mastrandrea^{70a,70b}, A. Mastroberardino^{40b,40a}, T. Masubuchi¹⁶⁰, T. Mathisen¹⁶⁸, A. Matic¹¹¹,
 N. Matsuzawa¹⁶⁰, J. Maurer^{26b}, B. Maček⁹⁰, D.A. Maximov^{118b,118a}, R. Mazini¹⁵⁵, I. Maznas¹⁵⁹,
 S.M. Mazza¹⁴², C. Mc Ginn²⁸, J.P. Mc Gowan¹⁰¹, S.P. Mc Kee¹⁰³, T.G. McCarthy¹¹², W.P. McCormack¹⁷,
 E.F. McDonald¹⁰², A.E. McDougall¹¹⁶, J.A. MCFayden¹⁵³, G. Mchedlidze^{156b}, M.A. McKay⁴¹,
 D.J. McLaughlin⁹³, K.D. McLean¹⁷², S.J. McMahan¹⁴⁰, P.C. McNamara¹⁰², R.A. McPherson^{172,v},
 J.E. Mdhluli^{32g}, Z.A. Meadows¹⁰⁰, S. Meehan³⁵, T. Megy³⁷, S. Mehlhase¹¹¹, A. Mehta⁸⁹, B. Meirose⁴²,
 D. Melini¹⁵⁷, B.R. Mellado Garcia^{32g}, A.H. Melo⁵², F. Meloni⁴⁵, A. Melzer²³, E.D. Mendes Gouveia^{136a},
 A.M. Mendes Jacques Da Costa²⁰, H.Y. Meng¹⁶³, L. Meng⁸⁸, S. Menke¹¹², M. Mentink³⁵, E. Meoni^{40b,40a},
 C. Merlassino¹³¹, P. Mermod^{53,*}, L. Merola^{68a,68b}, C. Meroni^{67a}, G. Merz¹⁰³, O. Meshkov^{108,110},
 J.K.R. Meshreki¹⁴⁸, J. Metcalfe⁵, A.S. Mete⁵, C. Meyer⁶⁴, J-P. Meyer¹⁴¹, M. Michetti¹⁸, R.P. Middleton¹⁴⁰,
 L. Mijovic⁴⁹, G. Mikenberg¹⁷⁶, M. Mikestikova¹³⁷, M. Mikuz⁹⁰, H. Mildner¹⁴⁶, A. Milic¹⁶³, C.D. Milke⁴¹,
 D.W. Miller³⁶, L.S. Miller³³, A. Milov¹⁷⁶, D.A. Milstead^{44a,44b}, T. Min^{14c}, A.A. Minaenko¹¹⁹,
 I.A. Minashvili^{156b}, L. Mince⁵⁶, A.I. Mincer¹²², B. Mindur^{82a}, M. Mineev⁷⁸, Y. Minegishi¹⁶⁰, Y. Mino⁸⁴,
 L.M. Mir¹³, M. Miralles Lopez¹⁷⁰, M. Mironova¹³¹, T. Mitani¹⁷⁵, A. Mitra¹⁷⁴, V.A. Mitsou¹⁷⁰, O. Miu¹⁶³,
 P.S. Miyagawa⁹¹, Y. Miyazaki⁸⁶, A. Mizukami⁸⁰, J.U. Mjörnmark⁹⁵, T. Mkrtchyan^{60a}, M. Mlynarikova¹¹⁷,
 T. Moa^{44a,44b}, S. Mobius⁵², K. Mochizuki¹⁰⁷, P. Moder⁴⁵, P. Mogg¹¹¹, A.F. Mohammed^{14a},
 S. Mohapatra³⁸, G. Mokgatitwane^{32g}, B. Mondal¹⁴⁸, S. Mondal¹³⁸, K. Mönig⁴⁵, E. Monnier⁹⁹,
 L. Monsonis Romero¹⁷⁰, J. Montejo Berlingen³⁵, M. Montella¹²⁴, F. Monticelli⁸⁷, N. Morange⁶³,
 A.L. Moreira De Carvalho^{136a}, M. Moreno Llácer¹⁷⁰, C. Moreno Martinez¹³, P. Morettini^{54b},
 S. Morgenstern¹⁷⁴, D. Mori¹⁴⁹, M. Morii⁵⁸, M. Morinaga¹⁶⁰, V. Morisbak¹³⁰, A.K. Morley³⁵,
 A.P. Morris⁹³, L. Morvaj³⁵, P. Moschovakos³⁵, B. Moser¹¹⁶, M. Mosidze^{156b}, T. Moskalets⁵¹,
 P. Moskvitina¹¹⁵, J. Moss^{30,m}, E.J.W. Moyses¹⁰⁰, S. Muanza⁹⁹, J. Mueller¹³⁵, R. Mueller¹⁹,
 D. Muenstermann⁸⁸, G.A. Mullier⁹⁵, J.J. Mullin¹³³, D.P. Mungo^{67a,67b}, J.L. Munoz Martinez¹³,
 F.J. Munoz Sanchez⁹⁸, M. Murin⁹⁸, P. Murin^{27b}, W.J. Murray^{174,140}, A. Murrone^{67a,67b}, J.M. Muse¹²⁵,
 M. Muškinja¹⁷, C. Mwewa²⁸, A.G. Myagkov^{119,ab}, A.J. Myers⁷, A.A. Myers¹³⁵, G. Myers⁶⁴, M. Myska¹³⁸,
 B.P. Nachman¹⁷, O. Nackenhurst⁴⁶, A.Nag Nag⁴⁷, K. Nagai¹³¹, K. Nagano⁸⁰, J.L. Nagle²⁸, E. Nagy⁹⁹,

A.M. Nairz³⁵, Y. Nakahama⁸⁰, K. Nakamura⁸⁰, H. Nanjo¹²⁹, F. Napolitano^{60a}, R. Narayan⁴¹,
 E.A. Narayanan¹¹⁴, I. Naryshkin¹³⁴, M. Naseri³³, C. Nass²³, G. Navarro^{21a}, J. Navarro-Gonzalez¹⁷⁰,
 R. Nayak¹⁵⁸, P.Y. Nechaeva¹⁰⁸, F. Nechansky⁴⁵, T.J. Neep²⁰, A. Negri^{69a,69b}, M. Negrini^{22b}, C. Nellist¹¹⁵,
 C. Nelson¹⁰¹, K. Nelson¹⁰³, S. Nemecek¹³⁷, M. Nessi^{35,f}, M.S. Neubauer¹⁶⁹, F. Neuhaus⁹⁷, J. Neundorff⁴⁵,
 R. Newhouse¹⁷¹, P.R. Newman²⁰, C.W. Ng¹³⁵, Y.S. Ng¹⁸, Y.W.Y. Ng¹⁶⁷, B. Ngair^{34e}, H.D.N. Nguyen¹⁰⁷,
 R.B. Nickerson¹³¹, R. Nicolaidou¹⁴¹, D.S. Nielsen³⁹, J. Nielsen¹⁴², M. Niemeyer⁵², N. Nikiforou¹⁰,
 V. Nikolaenko^{119,ab}, I. Nikolic-Audit¹³², K. Nikolopoulos²⁰, P. Nilsson²⁸, H.R. Nindhito⁵³, A. Nisati^{71a},
 N. Nishu², R. Nisius¹¹², T. Nitta¹⁷⁵, T. Nobe¹⁶⁰, D.L. Noel³¹, Y. Noguchi⁸⁴, I. Nomidis¹³²,
 M.A. Nomura²⁸, M.B. Norfolk¹⁴⁶, R.R.B. Norisam⁹³, J. Novak⁹⁰, T. Novak⁴⁵, O. Novgorodova⁴⁷,
 L. Novotny¹³⁸, R. Novotny¹¹⁴, L. Nozka¹²⁷, K. Ntekas¹⁶⁷, E. Nurse⁹³, F.G. Oakham^{33,af}, J. Ocariz¹³²,
 A. Ochi⁸¹, I. Ochoa^{136a}, J.P. Ochoa-Ricoux^{143a}, S. Oda⁸⁶, S. Odaka⁸⁰, S. Oerdek¹⁶⁸, A. Ogrodnik^{82a},
 A. Oh⁹⁸, C.C. Ohm¹⁵¹, H. Oide¹⁶¹, R. Oishi¹⁶⁰, M.L. Ojeda⁴⁵, Y. Okazaki⁸⁴, M.W. O'Keefe⁸⁹,
 Y. Okumura¹⁶⁰, A. Olariu^{26b}, L.F. Oleiro Seabra^{136a}, S.A. Olivares Pino^{143c}, D. Oliveira Damazio²⁸,
 D. Oliveira Goncalves^{79a}, J.L. Oliver¹⁶⁷, M.J.R. Olsson¹⁶⁷, A. Olszewski⁸³, J. Olszowska⁸³, Ö.O. Öncel²³,
 D.C. O'Neil¹⁴⁹, A.P. O'Neill¹⁹, A. Onofre^{136a,136e}, P.U.E. Onyisi¹⁰, R.G. Oreamuno Madriz¹¹⁷,
 M.J. Oreglia³⁶, G.E. Orellana⁸⁷, D. Orestano^{73a,73b}, N. Orlando¹³, R.S. Orr¹⁶³, V. O'Shea⁵⁶,
 R. Ospanov^{59a}, G. Otero y Garzon²⁹, H. Otono⁸⁶, P.S. Ott^{60a}, G.J. Ottino¹⁷, M. Ouchrif^{34d}, J. Ouellette²⁸,
 F. Ould-Saada¹³⁰, A. Ouraou^{141,*}, Q. Ouyang^{14a}, M. Owen⁵⁶, R.E. Owen¹⁴⁰, K.Y. Oyulmaz^{11c},
 V.E. Ozcan^{11c}, N. Ozturk⁷, S. Ozturk^{11c,z}, J. Pacalt¹²⁷, H.A. Pacey³¹, K. Pachal⁴⁸, A. Pacheco Pages¹³,
 C. Padilla Aranda¹³, S. Pagan Griso¹⁷, G. Palacino⁶⁴, S. Palazzo⁴⁹, S. Palestini³⁵, M. Palka^{82b}, J. Pan¹⁷⁹,
 D.K. Panchal¹⁰, C.E. Pandini⁵³, J.G. Panduro Vazquez⁹², P. Pani⁴⁵, G. Panizzo^{65a,65c}, L. Paolozzi⁵³,
 C. Papadatos¹⁰⁷, S. Parajuli⁴¹, A. Paramonov⁵, C. Paraskevopoulos⁹, D. Paredes Hernandez^{61b},
 B. Parida¹⁷⁶, T.H. Park¹⁶³, A.J. Parker³⁰, M.A. Parker³¹, F. Parodi^{54b,54a}, E.W. Parrish¹¹⁷, V.A. Parrish⁴⁹,
 J.A. Parsons³⁸, U. Parzefall⁵¹, L. Pascual Dominguez¹⁵⁸, V.R. Pascuzzi¹⁷, F. Pasquali¹¹⁶, E. Pasqualucci^{71a},
 S. Passaggio^{54b}, F. Pastore⁹², P. Pasuwan^{44a,44b}, J.R. Pater⁹⁸, A. Pathak¹⁷⁷, J. Patton⁸⁹, T. Pauly³⁵,
 J. Pearkes¹⁵⁰, M. Pedersen¹³⁰, R. Pedro^{136a}, S.V. Peleganchuk^{118b,118a}, O. Penc¹³⁷, C. Peng^{61b}, H. Peng^{59a},
 M. Penzin¹⁶², B.S. Peralva^{79a}, A.P. Pereira Peixoto^{136a}, L. Pereira Sanchez^{44a,44b}, D.V. Perepelitsa²⁸,
 E. Perez Codina^{164a}, M. Perganti⁹, L. Perini^{67a,67b}, H. Pernegger³⁵, S. Perrella³⁵, A. Perrevoort¹¹⁵,
 K. Peters⁴⁵, R.F.Y. Peters⁹⁸, B.A. Petersen³⁵, T.C. Petersen³⁹, E. Petit⁹⁹, V. Petousis¹³⁸, C. Petridou¹⁵⁹,
 A. Petrukhin¹⁴⁸, M. Pettee¹⁷, N.E. Pettersson³⁵, K. Petukhova¹³⁹, A. Peyaud¹⁴¹, R. Pezoa^{143f}, L. Pezzotti³⁵,
 G. Pezzullo¹⁷⁹, T. Pham¹⁰², P.W. Phillips¹⁴⁰, M.W. Phipps¹⁶⁹, G. Piacquadio¹⁵², E. Pianori¹⁷,
 F. Piazza^{67a,67b}, R. Piegai²⁹, D. Pietreanu^{26b}, A.D. Pilkington⁹⁸, M. Pinamonti^{65a,65c}, J.L. Pinfold²,
 C. Pitman Donaldson⁹³, D.A. Pizzi³³, L. Pizzimento^{72a,72b}, A. Pizzini¹¹⁶, M.-A. Pleier²⁸, V. Plesanovs⁵¹,
 V. Pleskot¹³⁹, E. Plotnikova⁷⁸, R. Poettgen⁹⁵, R. Poggi⁵³, L. Poggioli¹³², I. Pogrebnyak¹⁰⁴, D. Pohl²³,
 I. Pokharel⁵², G. Polesello^{69a}, A. Poley^{149,164a}, R. Polifka¹³⁸, A. Polini^{22b}, C.S. Pollard¹³¹, Z.B. Pollock¹²⁴,
 V. Polychronakos²⁸, D. Ponomarenko¹⁰⁹, L. Pontecorvo³⁵, S. Popa^{26a}, G.A. Popeneciu^{26d}, L. Portales⁴,
 D.M. Portillo Quintero^{164a}, S. Pospisil¹³⁸, P. Postolache^{26c}, K. Potamianos¹³¹, I.N. Potrap⁷⁸, C.J. Potter³¹,
 H. Potti¹, T. Poulsen⁴⁵, J. Poveda¹⁷⁰, T.D. Powell¹⁴⁶, G. Pownall⁴⁵, M.E. Pozo Astigarraga³⁵,
 A. Prades Ibanez¹⁷⁰, P. Pralavorio⁹⁹, M.M. Prapa⁴³, D. Price⁹⁸, M. Primavera^{66a}, M.A. Principe Martin⁹⁶,
 M.L. Proffitt¹⁴⁵, N. Proklova¹⁰⁹, K. Prokofiev^{61c}, F. Prokoshin⁷⁸, G. Proto^{72a,72b}, S. Protopopescu²⁸,
 J. Proudfoot⁵, M. Przybycien^{82a}, D. Pudzha¹³⁴, P. Puzo⁶³, D. Pyatiizbyantseva¹⁰⁹, J. Qian¹⁰³, Y. Qin⁹⁸,
 T. Qiu⁹¹, A. Quadri⁵², M. Queitsch-Maitland³⁵, G. Rabanal Bolanos⁵⁸, F. Ragusa^{67a,67b}, J.A. Raine⁵³,
 S. Rajagopalan²⁸, K. Ran^{14a,14d}, D.F. Rassloff^{60a}, S. Rave⁹⁷, B. Ravina⁵⁶, I. Ravinovich¹⁷⁶, M. Raymond³⁵,
 A.L. Read¹³⁰, N.P. Readioff¹⁴⁶, D.M. Rebutti^{69a,69b}, G. Redlinger²⁸, K. Reeves⁴², D. Reikher¹⁵⁸,
 A. Reiss⁹⁷, A. Rej¹⁴⁸, C. Rembser³⁵, A. Renardi⁴⁵, M. Renda^{26b}, M.B. Rendel¹¹², A.G. Rennie⁵⁶,
 S. Resconi^{67a}, M. Ressegotti^{54b,54a}, E.D. Resseguie¹⁷, S. Rettie⁹³, B. Reynolds¹²⁴, E. Reynolds¹⁷,
 M. Rezaei Estabragh¹⁷⁸, O.L. Rezanova^{118b,118a}, P. Reznicek¹³⁹, E. Ricci^{74a,74b}, R. Richter¹¹², S. Richter⁴⁵,

E. Richter-Was^{82b}, M. Ridel¹³², P. Rieck¹²², P. Riedler³⁵, M. Rijssenbeek¹⁵², A. Rimoldi^{69a,69b},
 M. Rimoldi⁴⁵, L. Rinaldi^{22b,22a}, T.T. Rinn¹⁶⁹, M.P. Rinnagel¹¹¹, G. Ripellino¹⁵¹, I. Riu¹³, P. Rivadeneira⁴⁵,
 J.C. Rivera Vergara¹⁷², F. Rizatdinova¹²⁶, E. Rizvi⁹¹, C. Rizzi⁵³, B.A. Roberts¹⁷⁴, B.R. Roberts¹⁷,
 S.H. Robertson^{101,v}, M. Robin⁴⁵, D. Robinson³¹, C.M. Robles Gajardo^{143f}, M. Robles Manzano⁹⁷,
 A. Robson⁵⁶, A. Rocchi^{72a,72b}, C. Roda^{70a,70b}, S. Rodriguez Bosca^{60a}, Y. Rodriguez Garcia^{21a},
 A. Rodriguez Rodriguez⁵¹, A.M. Rodríguez Vera^{164b}, S. Roe³⁵, A.R. Roepe¹²⁵, J. Roggel¹⁷⁸, O. Røhne¹³⁰,
 R.A. Rojas¹⁷², B. Roland⁵¹, C.P.A. Roland⁶⁴, J. Roloff²⁸, A. Romaniouk¹⁰⁹, M. Romano^{22b},
 A.C. Romero Hernandez¹⁶⁹, N. Rompotis⁸⁹, M. Ronzani¹²², L. Roos¹³², S. Rosati^{71a}, B.J. Rosser¹³³,
 E. Rossi¹⁶³, E. Rossi⁴, E. Rossi^{68a,68b}, L.P. Rossi^{54b}, L. Rossini⁴⁵, R. Rosten¹²⁴, M. Rotaru^{26b}, B. Rottler⁵¹,
 D. Rousseau⁶³, D. Rouso³¹, G. Rovelli^{69a,69b}, A. Roy¹⁰, A. Rozanov⁹⁹, Y. Rozen¹⁵⁷, X. Ruan^{32g},
 A.J. Ruby⁸⁹, T.A. Ruggeri¹, F. Rühr⁵¹, A. Ruiz-Martinez¹⁷⁰, A. Rummler³⁵, Z. Rurikova⁵¹,
 N.A. Rusakovich⁷⁸, H.L. Russell¹⁷², L. Rustige³⁷, J.P. Rutherford⁶, E.M. Rüttinger¹⁴⁶, K. Rybacki⁸⁸,
 M. Rybar¹³⁹, E.B. Rye¹³⁰, A. Ryzhov¹¹⁹, J.A. Sabater Iglesias⁵³, P. Sabatini¹⁷⁰, L. Sabetta^{71a,71b},
 H.F-W. Sadrozinski¹⁴², R. Sadykov⁷⁸, F. Safai Tehrani^{71a}, B. Safarzadeh Samani¹⁵³, M. Safdari¹⁵⁰,
 S. Saha¹⁰¹, M. Sahinsoy¹¹², A. Sahu¹⁷⁸, M. Saimpert¹⁴¹, M. Saito¹⁶⁰, T. Saito¹⁶⁰, D. Salamani³⁵,
 G. Salamanna^{73a,73b}, A. Salnikov¹⁵⁰, J. Salt¹⁷⁰, A. Salvador Salas¹³, D. Salvatore^{40b,40a}, F. Salvatore¹⁵³,
 A. Salzburger³⁵, D. Sammel⁵¹, D. Sampsonidis¹⁵⁹, D. Sampsonidou^{59d,59c}, J. Sánchez¹⁷⁰,
 A. Sanchez Pineda⁴, V. Sanchez Sebastian¹⁷⁰, H. Sandaker¹³⁰, C.O. Sander⁴⁵, I.G. Sanderswood⁸⁸,
 J.A. Sandesara¹⁰⁰, M. Sandhoff¹⁷⁸, C. Sandoval^{21b}, D.P.C. Sankey¹⁴⁰, A. Sansoni⁵⁰, C. Santoni³⁷,
 H. Santos^{136a,136b}, S.N. Santpur¹⁷, A. Santra¹⁷⁶, K.A. Saoucha¹⁴⁶, A. Sapronov⁷⁸, J.G. Saraiva^{136a,136d},
 J. Sardain⁹⁹, O. Sasaki⁸⁰, K. Sato¹⁶⁵, C. Sauer^{60b}, F. Sauerburger⁵¹, E. Sauvan⁴, P. Savard^{163,af},
 R. Sawada¹⁶⁰, C. Sawyer¹⁴⁰, L. Sawyer⁹⁴, I. Sayago Galvan¹⁷⁰, C. Sbarra^{22b}, A. Sbrizzi^{22b,22a},
 T. Scanlon⁹³, J. Schaarschmidt¹⁴⁵, P. Schacht¹¹², D. Schaefer³⁶, U. Schäfer⁹⁷, A.C. Schaffer⁶³,
 D. Schaile¹¹¹, R.D. Schamberger¹⁵², E. Schanet¹¹¹, C. Scharf¹⁸, N. Scharmberg⁹⁸, V.A. Schegelsky¹³⁴,
 D. Scheirich¹³⁹, F. Schenck¹⁸, M. Schernau¹⁶⁷, C. Schiavi^{54b,54a}, Z.M. Schillaci²⁵, E.J. Schioppa^{66a,66b},
 M. Schioppa^{40b,40a}, B. Schlag⁹⁷, K.E. Schleicher⁵¹, S. Schlenker³⁵, K. Schmieden⁹⁷, C. Schmitt⁹⁷,
 S. Schmitt⁴⁵, L. Schoeffel¹⁴¹, A. Schoening^{60b}, P.G. Scholer⁵¹, E. Schopf¹³¹, M. Schott⁹⁷,
 J. Schovancova³⁵, S. Schramm⁵³, F. Schroeder¹⁷⁸, H-C. Schultz-Coulon^{60a}, M. Schumacher⁵¹,
 B.A. Schumm¹⁴², Ph. Schune¹⁴¹, A. Schwartzman¹⁵⁰, T.A. Schwarz¹⁰³, Ph. Schwemling¹⁴¹,
 R. Schwienhorst¹⁰⁴, A. Sciandra¹⁴², G. Sciolla²⁵, F. Scuri^{70a}, F. Scutti¹⁰², C.D. Sebastiani⁸⁹,
 K. Sedlaczek⁴⁶, P. Seema¹⁸, S.C. Seidel¹¹⁴, A. Seiden¹⁴², B.D. Seidlitz²⁸, T. Seiss³⁶, C. Seitz⁴⁵,
 J.M. Seixas^{79b}, G. Sekhniaidze^{68a}, S.J. Sekula⁴¹, L.P. Selem⁴, N. Semprini-Cesari^{22b,22a}, S. Sen⁴⁸,
 L. Serin⁶³, L. Serkin^{65a,65b}, M. Sessa^{73a,73b}, H. Severini¹²⁵, S. Sevova¹⁵⁰, F. Sforza^{54b,54a}, A. Sfyrly⁵³,
 E. Shabalina⁵², R. Shaheen¹⁵¹, J.D. Shahinian¹³³, N.W. Shaikh^{44a,44b}, D. Shaked Renous¹⁷⁶, L.Y. Shan^{14a},
 M. Shapiro¹⁷, A. Sharma³⁵, A.S. Sharma¹, S. Sharma⁴⁵, P.B. Shatalov¹²⁰, K. Shaw¹⁵³, S.M. Shaw⁹⁸,
 P. Sherwood⁹³, L. Shi⁹³, C.O. Shimmin¹⁷⁹, Y. Shimogama¹⁷⁵, J.D. Shinner⁹², I.P.J. Shipsey¹³¹,
 S. Shirabe⁵³, M. Shiyakova⁷⁸, J. Shlomi¹⁷⁶, M.J. Shochet³⁶, J. Shojaii¹⁰², D.R. Shope¹⁵¹, S. Shrestha¹²⁴,
 E.M. Shrif^{32g}, M.J. Shroff¹⁷², E. Shulga¹⁷⁶, P. Sicho¹³⁷, A.M. Sickles¹⁶⁹, E. Sideras Haddad^{32g},
 O. Sidiropoulou³⁵, A. Sidoti^{22b}, F. Siegert⁴⁷, Dj. Sijacki¹⁵, F. Sili⁸⁷, J.M. Silva²⁰, M.V. Silva Oliveira³⁵,
 S.B. Silverstein^{44a}, S. Simion⁶³, R. Simoniello³⁵, N.D. Simpson⁹⁵, S. Simsek^{11c}, S. Sindhu⁵²,
 P. Sinervo¹⁶³, V. Sinetckii¹¹⁰, S. Singh¹⁴⁹, S. Singh¹⁶³, S. Sinha⁴⁵, S. Sinha^{32g}, M. Sioli^{22b,22a}, I. Siral¹²⁸,
 S.Yu. Sivoklokov¹¹⁰, J. Sjölin^{44a,44b}, A. Skaf⁵², E. Skorda⁹⁵, P. Skubic¹²⁵, M. Slawinska⁸³, V. Smakhtin¹⁷⁶,
 B.H. Smart¹⁴⁰, J. Smiesko¹³⁹, S.Yu. Smirnov¹⁰⁹, Y. Smirnov¹⁰⁹, L.N. Smirnova^{110,q}, O. Smirnova⁹⁵,
 E.A. Smith³⁶, H.A. Smith¹³¹, M. Smizanska⁸⁸, K. Smolek¹³⁸, A. Smykiewicz⁸³, A.A. Snesev¹⁰⁸,
 H.L. Snoek¹¹⁶, S. Snyder²⁸, R. Sobie^{172,v}, A. Soffer¹⁵⁸, C.A. Solans Sanchez³⁵, E.Yu. Soldatov¹⁰⁹,
 U. Soldevila¹⁷⁰, A.A. Solodkov¹¹⁹, S. Solomon⁵¹, A. Soloshenko⁷⁸, K. Solovieva⁵¹, O.V. Solovyanov¹¹⁹,
 V. Solovyev¹³⁴, P. Sommer¹⁴⁶, H. Son¹⁶⁶, A. Sonay¹³, W.Y. Song^{164b}, A. Sopczak¹³⁸, A.L. Soppio⁹³,

F. Sopkova^{27b}, S. Sottocornola^{69a,69b}, R. Soualah^{121c}, A.M. Soukharev^{118b,118a}, Z. Soumami^{34e}, D. South⁴⁵, S. Spagnolo^{66a,66b}, M. Spalla¹¹², M. Spangenberg¹⁷⁴, F. Spanò⁹², D. Sperlich⁵¹, G. Spigo³⁵, M. Spina¹⁵³, S. Spinali⁸⁸, D.P. Spiteri⁵⁶, M. Spousta¹³⁹, A. Stabile^{67a,67b}, B.L. Stamas¹¹⁷, R. Stamen^{60a}, M. Stamenkovic¹¹⁶, A. Stampekis²⁰, M. Standke²³, E. Stanecka⁸³, B. Stanislaus¹⁷, M.M. Stanitzki⁴⁵, M. Stankaityte¹³¹, B. Stapf⁴⁵, E.A. Starchenko¹¹⁹, G.H. Stark¹⁴², J. Stark⁹⁹, D.M. Starko^{164b}, P. Staroba¹³⁷, P. Starovoitov^{60a}, S. Stärz¹⁰¹, R. Staszewski⁸³, G. Stavropoulos⁴³, P. Steinberg²⁸, A.L. Steinhebel¹²⁸, B. Stelzer^{149,164a}, H.J. Stelzer¹³⁵, O. Stelzer-Chilton^{164a}, H. Stenzel⁵⁵, T.J. Stevenson¹⁵³, G.A. Stewart³⁵, M.C. Stockton³⁵, G. Stoicea^{26b}, M. Stolarski^{136a}, S. Stonjek¹¹², A. Straessner⁴⁷, J. Strandberg¹⁵¹, S. Strandberg^{44a,44b}, M. Strauss¹²⁵, T. Strebler⁹⁹, P. Strizenc^{27b}, R. Ströhmer¹⁷³, D.M. Strom¹²⁸, L.R. Strom⁴⁵, R. Stroynowski⁴¹, A. Strubig^{44a,44b}, S.A. Stucci²⁸, B. Stugu¹⁶, J. Stupak¹²⁵, N.A. Styles⁴⁵, D. Su¹⁵⁰, S. Su^{59a}, W. Su^{59d,145,59c}, X. Su^{59a}, K. Sugizaki¹⁶⁰, V.V. Sulin¹⁰⁸, M.J. Sullivan⁸⁹, D.M.S. Sultan^{74a,74b}, L. Sultanaliyeva¹⁰⁸, S. Sultansoy^{3c}, T. Sumida⁸⁴, S. Sun¹⁰³, S. Sun¹⁷⁷, O. Sunneborn Gudnadottir¹⁶⁸, M.R. Sutton¹⁵³, M. Svatos¹³⁷, M. Swiatlowski^{164a}, T. Swirski¹⁷³, I. Sykora^{27a}, M. Sykora¹³⁹, T. Sykora¹³⁹, D. Ta⁹⁷, K. Tackmann^{45,u}, A. Taffard¹⁶⁷, R. Tafirout^{164a}, R.H.M. Taibah¹³², R. Takashima⁸⁵, K. Takeda⁸¹, E.P. Takeva⁴⁹, Y. Takubo⁸⁰, M. Talby⁹⁹, A.A. Talyshev^{118b,118a}, K.C. Tam^{61b}, N.M. Tamir¹⁵⁸, A. Tanaka¹⁶⁰, J. Tanaka¹⁶⁰, R. Tanaka⁶³, J. Tang^{59c}, Z. Tao¹⁷¹, S. Tapia Araya⁷⁷, S. Tapprogge⁹⁷, A. Tarek Abouelfadl Mohamed¹⁰⁴, S. Tarem¹⁵⁷, K. Tariq^{59b}, G. Tarna^{26b}, G.F. Tartarelli^{67a}, P. Tas¹³⁹, M. Tasevsky¹³⁷, E. Tassi^{40b,40a}, G. Tateno¹⁶⁰, Y. Tayalati^{34e}, G.N. Taylor¹⁰², W. Taylor^{164b}, H. Teagle⁸⁹, A.S. Tee¹⁷⁷, R. Teixeira De Lima¹⁵⁰, P. Teixeira-Dias⁹², J.J. Teoh¹¹⁶, K. Terashi¹⁶⁰, J. Terron⁹⁶, S. Terzo¹³, M. Testa⁵⁰, R.J. Teuscher^{163,v}, N. Themistokleous⁴⁹, T. Thevenaux-Pelzer¹⁸, O. Thielmann¹⁷⁸, D.W. Thomas⁹², J.P. Thomas²⁰, E.A. Thompson⁴⁵, P.D. Thompson²⁰, E. Thomson¹³³, E.J. Thorpe⁹¹, Y. Tian⁵², V.O. Tikhomirov^{108,ac}, Yu.A. Tikhonov^{118b,118a}, S. Timoshenko¹⁰⁹, E.X.L. Ting¹, P. Tipton¹⁷⁹, S. Tisserant⁹⁹, S.H. Tlou^{32g}, A. Tmourji³⁷, K. Todome^{22b,22a}, S. Todorova-Nova¹³⁹, S. Todt⁴⁷, M. Togawa⁸⁰, J. Tojo⁸⁶, S. Tokár^{27a}, K. Tokushuku⁸⁰, R. Tombs³¹, M. Tomoto^{80,113}, L. Tompkins¹⁵⁰, P. Tornambe¹⁰⁰, E. Torrence¹²⁸, H. Torres⁴⁷, E. Torró Pastor¹⁷⁰, M. Toscani²⁹, C. Toscirì³⁶, D.R. Tovey¹⁴⁶, A. Traet¹⁶, I.S. Trandafir^{26b}, C.J. Treado¹²², T. Trefzger¹⁷³, A. Tricoli²⁸, I.M. Trigger^{164a}, S. Trincaz-Duvoid¹³², D.A. Trischuk¹⁷¹, W. Trischuk¹⁶³, B. Trocmé⁵⁷, A. Trofymov⁶³, C. Troncon^{67a}, F. Trovato¹⁵³, L. Truong^{32c}, M. Trzebinski⁸³, A. Trzupek⁸³, F. Tsai¹⁵², M. Tsai¹⁰³, A. Tsiamis¹⁵⁹, P.V. Tsiarehsha¹⁰⁵, A. Tsirigotis^{159,s}, V. Tsiskaridze¹⁵², E.G. Tskhadadze^{156a}, M. Tsopoulou¹⁵⁹, Y. Tsujikawa⁸⁴, I.I. Tsukerman¹²⁰, V. Tsulaia¹⁷, S. Tsuno⁸⁰, O. Tsur¹⁵⁷, D. Tsybychev¹⁵², Y. Tu^{61b}, A. Tudorache^{26b}, V. Tudorache^{26b}, A.N. Tuna³⁵, S. Turchikhin⁷⁸, I. Turk Cakir^{3a}, R. Turra^{67a}, P.M. Tuts³⁸, S. Tzamarias¹⁵⁹, P. Tzani⁹, E. Tzovara⁹⁷, K. Uchida¹⁶⁰, F. Ukegawa¹⁶⁵, P.A. Ulloa Poblete^{143c}, G. Unal³⁵, M. Unal¹⁰, A. Undrus²⁸, G. Unel¹⁶⁷, K. Uno¹⁶⁰, J. Urban^{27b}, P. Urquijo¹⁰², G. Usai⁷, R. Ushioda¹⁶¹, M. Usman¹⁰⁷, Z. Uysal^{11d}, V. Vacek¹³⁸, B. Vachon¹⁰¹, K.O.H. Vadla¹³⁰, T. Vafeiadis³⁵, C. Valderanis¹¹¹, E. Valdes Santurio^{44a,44b}, M. Valente^{164a}, S. Valentinetti^{22b,22a}, A. Valero¹⁷⁰, A. Vallier⁹⁹, J.A. Valls Ferrer¹⁷⁰, T.R. Van Daalen¹⁴⁵, P. Van Gemmeren⁵, S. Van Stroud⁹³, I. Van Vulpen¹¹⁶, M. Vanadia^{72a,72b}, W. Vandelli³⁵, M. Vandenbroucke¹⁴¹, E.R. Vandewall¹²⁶, D. Vannicola¹⁵⁸, L. Vannoli^{54b,54a}, R. Vari^{71a}, E.W. Varnes⁶, C. Varni¹⁷, T. Varol¹⁵⁵, D. Varouchas⁶³, K.E. Varvell¹⁵⁴, M.E. Vasile^{26b}, L. Vaslin³⁷, G.A. Vasquez¹⁷², F. Vazeille³⁷, D. Vazquez Furelos¹³, T. Vazquez Schroeder³⁵, J. Veatch⁵², V. Vecchio⁹⁸, M.J. Veen¹¹⁶, I. Veliscek¹³¹, L.M. Veloce¹⁶³, F. Veloso^{136a,136c}, S. Veneziano^{71a}, A. Ventura^{66a,66b}, A. Verbitskyi¹¹², M. Verducci^{70a,70b}, C. Vergis²³, M. Verissimo De Araujo^{79b}, W. Verkerke¹¹⁶, J.C. Vermeulen¹¹⁶, C. Vernieri¹⁵⁰, P.J. Verschuuren⁹², M. Vessella¹⁰⁰, M.L. Vesterbacka¹²², M.C. Vetterli^{149,af}, A. Vgenopoulos¹⁵⁹, N. Viaux Maira^{143f}, T. Vickey¹⁴⁶, O.E. Vickey Boeriu¹⁴⁶, G.H.A. Viehhauser¹³¹, L. Vigani^{60b}, M. Villa^{22b,22a}, M. Villaplana Perez¹⁷⁰, E.M. Villhauer⁴⁹, E. Vilucchi⁵⁰, M.G. Vinciter³³, G.S. Virdee²⁰, A. Vishwakarma⁴⁹, C. Vittori^{22b,22a}, I. Vivarelli¹⁵³, V. Vladimirov¹⁷⁴, E. Voevodina¹¹², M. Vogel¹⁷⁸, P. Vokac¹³⁸, J. Von Ahnen⁴⁵, E. Von Toerne²³, B. Vormwald³⁵, V. Vorobel¹³⁹, K. Vorobev¹⁰⁹,

M. Vos¹⁷⁰, J.H. Vosseveld⁸⁹, M. Vozak⁹⁸, L. Vozdecky⁹¹, N. Vranjes¹⁵, M. Vranjes Milosavljevic¹⁵, V. Vrba^{138,*}, M. Vreeswijk¹¹⁶, N.K. Vu⁹⁹, R. Vuillermet³⁵, O.V. Vujinovic⁹⁷, I. Vukotic³⁶, S. Wada¹⁶⁵, C. Wagner¹⁰⁰, W. Wagner¹⁷⁸, S. Wahdan¹⁷⁸, H. Wahlberg⁸⁷, R. Wakasa¹⁶⁵, M. Wakida¹¹³, V.M. Walbrecht¹¹², J. Walder¹⁴⁰, R. Walker¹¹¹, S.D. Walker⁹², W. Walkowiak¹⁴⁸, A.M. Wang⁵⁸, A.Z. Wang¹⁷⁷, C. Wang^{59a}, C. Wang^{59c}, H. Wang¹⁷, J. Wang^{61a}, P. Wang⁴¹, R.-J. Wang⁹⁷, R. Wang⁵⁸, R. Wang⁵, S.M. Wang¹⁵⁵, S. Wang^{59b}, T. Wang^{59a}, W.T. Wang⁷⁶, W.X. Wang^{59a}, X. Wang^{14c}, X. Wang¹⁶⁹, X. Wang^{59c}, Y. Wang^{59a}, Z. Wang¹⁰³, Z. Wang^{59d,48,59c}, Z. Wang¹⁰³, A. Warburton¹⁰¹, R.J. Ward²⁰, N. Warrack⁵⁶, A.T. Watson²⁰, M.F. Watson²⁰, G. Watts¹⁴⁵, B.M. Waugh⁹³, A.F. Webb¹⁰, C. Weber²⁸, M.S. Weber¹⁹, S.A. Weber³³, S.M. Weber^{60a}, C. Wei^{59a}, Y. Wei¹³¹, A.R. Weidberg¹³¹, J. Weingarten⁴⁶, M. Weirich⁹⁷, C. Weiser⁵¹, T. Wenaus²⁸, B. Wendland⁴⁶, T. Wengler³⁵, N. Wermes²³, M. Wessels^{60a}, K. Whalen¹²⁸, A.M. Wharton⁸⁸, A.S. White⁵⁸, A. White⁷, M.J. White¹, D. Whiteson¹⁶⁷, L. Wickremasinghe¹²⁹, W. Wiedenmann¹⁷⁷, C. Wiel⁴⁷, M. Wielers¹⁴⁰, N. Wieseotte⁹⁷, C. Wiglesworth³⁹, L.A.M. Wiik-Fuchs⁵¹, D.J. Wilbern¹²⁵, H.G. Wilkens³⁵, L.J. Wilkins⁹², D.M. Williams³⁸, H.H. Williams¹³³, S. Williams³¹, S. Willocq¹⁰⁰, P.J. Windischhofer¹³¹, F. Winklmeier¹²⁸, B.T. Winter⁵¹, M. Wittgen¹⁵⁰, M. Wobisch⁹⁴, A. Wolf⁹⁷, R. Wölker¹³¹, J. Wollrath¹⁶⁷, M.W. Wolter⁸³, H. Wolters^{136a,136c}, V.W.S. Wong¹⁷¹, A.F. Wongel⁴⁵, S.D. Worm⁴⁵, B.K. Wosiek⁸³, K.W. Woźniak⁸³, K. Wraight⁵⁶, J. Wu^{14a,14d}, S.L. Wu¹⁷⁷, X. Wu⁵³, Y. Wu^{59a}, Z. Wu^{141,59a}, J. Wuerzinger¹³¹, T.R. Wyatt⁹⁸, B.M. Wynne⁴⁹, S. Xella³⁹, L. Xia^{14c}, M. Xia^{14b}, J. Xiang^{61c}, X. Xiao¹⁰³, M. Xie^{59a}, X. Xie^{59a}, I. Xiotidis¹⁵³, D. Xu^{14a}, H. Xu^{59a}, H. Xu^{59a}, L. Xu^{59a}, R. Xu¹³³, T. Xu^{59a}, W. Xu¹⁰³, Y. Xu^{14b}, Z. Xu^{59b}, Z. Xu¹⁵⁰, B. Yabsley¹⁵⁴, S. Yacoub^{32a}, N. Yamaguchi⁸⁶, Y. Yamaguchi¹⁶¹, H. Yamauchi¹⁶⁵, T. Yamazaki¹⁷, Y. Yamazaki⁸¹, J. Yan^{59c}, S. Yan¹³¹, Z. Yan²⁴, H.J. Yang^{59c,59d}, H.T. Yang¹⁷, S. Yang^{59a}, T. Yang^{61c}, X. Yang^{59a}, X. Yang^{14a}, Y. Yang¹⁶⁰, Z. Yang^{103,59a}, W.-M. Yao¹⁷, Y.C. Yap⁴⁵, H. Ye^{14c}, J. Ye⁴¹, S. Ye²⁸, I. Yeletsikh⁷⁸, M.R. Yexley⁸⁸, P. Yin³⁸, K. Yorita¹⁷⁵, C.J.S. Young⁵¹, C. Young¹⁵⁰, M. Yuan¹⁰³, R. Yuan^{59b,i}, X. Yue^{60a}, M. Zaazoua^{34e}, B. Zabinski⁸³, G. Zacharis⁹, E. Zaid⁴⁹, A.M. Zaitsev^{119,ab}, T. Zakareishvili^{156b}, N. Zakharchuk³³, S. Zambito³⁵, D. Zanzi⁵¹, O. Zaplatilek¹³⁸, S.V. Zeibner⁴⁶, C. Zeitnitz¹⁷⁸, J.C. Zeng¹⁶⁹, D.T. Zenger Jr²⁵, O. Zenin¹¹⁹, T. Ženiš^{27a}, S. Zenz⁹¹, S. Zerradi^{34a}, D. Zerwas⁶³, B. Zhang^{14c}, D.F. Zhang¹⁴⁶, G. Zhang^{14b}, J. Zhang⁵, K. Zhang^{14a}, L. Zhang^{14c}, M. Zhang¹⁶⁹, R. Zhang¹⁷⁷, S. Zhang¹⁰³, X. Zhang^{59c}, X. Zhang^{59b}, Z. Zhang⁶³, H. Zhao¹⁴⁵, P. Zhao⁴⁸, T. Zhao^{59b}, Y. Zhao¹⁴², Z. Zhao^{59a}, A. Zhemchugov⁷⁸, Z. Zheng¹⁵⁰, D. Zhong¹⁶⁹, B. Zhou¹⁰³, C. Zhou¹⁷⁷, H. Zhou⁶, N. Zhou^{59c}, Y. Zhou⁶, C.G. Zhu^{59b}, C. Zhu^{14a,14d}, H.L. Zhu^{59a}, H. Zhu^{14a}, J. Zhu¹⁰³, Y. Zhu^{59a}, X. Zhuang^{14a}, K. Zhukov¹⁰⁸, V. Zhulanov^{118b,118a}, D. Zieminska⁶⁴, N.I. Zimine⁷⁸, S. Zimmermann^{51,*}, J. Zinsser^{60b}, M. Ziolkowski¹⁴⁸, L. Živković¹⁵, A. Zoccoli^{22b,22a}, K. Zoch⁵³, T.G. Zorbas¹⁴⁶, O. Zormpa⁴³, W. Zou³⁸, L. Zwalinski³⁵.

¹Department of Physics, University of Adelaide, Adelaide; Australia.

²Department of Physics, University of Alberta, Edmonton AB; Canada.

³(*a*) Department of Physics, Ankara University, Ankara; (*b*) Istanbul Aydin University, Application and Research Center for Advanced Studies, Istanbul; (*c*) Division of Physics, TOBB University of Economics and Technology, Ankara; Turkey.

⁴LAPP, Univ. Savoie Mont Blanc, CNRS/IN2P3, Annecy ; France.

⁵High Energy Physics Division, Argonne National Laboratory, Argonne IL; United States of America.

⁶Department of Physics, University of Arizona, Tucson AZ; United States of America.

⁷Department of Physics, University of Texas at Arlington, Arlington TX; United States of America.

⁸Physics Department, National and Kapodistrian University of Athens, Athens; Greece.

⁹Physics Department, National Technical University of Athens, Zografou; Greece.

¹⁰Department of Physics, University of Texas at Austin, Austin TX; United States of America.

¹¹(*a*) Bahcesehir University, Faculty of Engineering and Natural Sciences, Istanbul; (*b*) Istanbul Bilgi University, Faculty of Engineering and Natural Sciences, Istanbul; (*c*) Department of Physics, Bogazici

University, Istanbul;^(d) Department of Physics Engineering, Gaziantep University, Gaziantep;^(e) Department of Physics, Istanbul University, Istanbul;^(f) Istinye University, Sariyer, Istanbul; Turkey.

¹² Institute of Physics, Azerbaijan Academy of Sciences, Baku; Azerbaijan.

¹³ Institut de Física d'Altes Energies (IFAE), Barcelona Institute of Science and Technology, Barcelona; Spain.

¹⁴(^a) Institute of High Energy Physics, Chinese Academy of Sciences, Beijing;^(b) Physics Department, Tsinghua University, Beijing;^(c) Department of Physics, Nanjing University, Nanjing;^(d) University of Chinese Academy of Science (UCAS), Beijing; China.

¹⁵ Institute of Physics, University of Belgrade, Belgrade; Serbia.

¹⁶ Department for Physics and Technology, University of Bergen, Bergen; Norway.

¹⁷ Physics Division, Lawrence Berkeley National Laboratory and University of California, Berkeley CA; United States of America.

¹⁸ Institut für Physik, Humboldt Universität zu Berlin, Berlin; Germany.

¹⁹ Albert Einstein Center for Fundamental Physics and Laboratory for High Energy Physics, University of Bern, Bern; Switzerland.

²⁰ School of Physics and Astronomy, University of Birmingham, Birmingham; United Kingdom.

²¹(^a) Facultad de Ciencias y Centro de Investigaciones, Universidad Antonio Nariño, Bogotá;^(b) Departamento de Física, Universidad Nacional de Colombia, Bogotá; Colombia.

²²(^a) Dipartimento di Fisica e Astronomia A. Righi, Università di Bologna, Bologna;^(b) INFN Sezione di Bologna; Italy.

²³ Physikalisches Institut, Universität Bonn, Bonn; Germany.

²⁴ Department of Physics, Boston University, Boston MA; United States of America.

²⁵ Department of Physics, Brandeis University, Waltham MA; United States of America.

²⁶(^a) Transilvania University of Brasov, Brasov;^(b) Horia Hulubei National Institute of Physics and Nuclear Engineering, Bucharest;^(c) Department of Physics, Alexandru Ioan Cuza University of Iasi, Iasi;^(d) National Institute for Research and Development of Isotopic and Molecular Technologies, Physics Department, Cluj-Napoca;^(e) University Politehnica Bucharest, Bucharest;^(f) West University in Timisoara, Timisoara; Romania.

²⁷(^a) Faculty of Mathematics, Physics and Informatics, Comenius University, Bratislava;^(b) Department of Subnuclear Physics, Institute of Experimental Physics of the Slovak Academy of Sciences, Kosice; Slovak Republic.

²⁸ Physics Department, Brookhaven National Laboratory, Upton NY; United States of America.

²⁹ Departamento de Física (FCEN) and IFIBA, Universidad de Buenos Aires and CONICET, Buenos Aires; Argentina.

³⁰ California State University, CA; United States of America.

³¹ Cavendish Laboratory, University of Cambridge, Cambridge; United Kingdom.

³²(^a) Department of Physics, University of Cape Town, Cape Town;^(b) iThemba Labs, Western Cape;^(c) Department of Mechanical Engineering Science, University of Johannesburg, Johannesburg;^(d) National Institute of Physics, University of the Philippines Diliman (Philippines);^(e) University of South Africa, Department of Physics, Pretoria;^(f) University of Zululand, KwaDlangezwa;^(g) School of Physics, University of the Witwatersrand, Johannesburg; South Africa.

³³ Department of Physics, Carleton University, Ottawa ON; Canada.

³⁴(^a) Faculté des Sciences Ain Chock, Réseau Universitaire de Physique des Hautes Energies - Université Hassan II, Casablanca;^(b) Faculté des Sciences, Université Ibn-Tofail, Kénitra;^(c) Faculté des Sciences Semlalia, Université Cadi Ayyad, LPHEA-Marrakech;^(d) LPMR, Faculté des Sciences, Université Mohamed Premier, Oujda;^(e) Faculté des sciences, Université Mohammed V, Rabat;^(f) Mohammed VI

Polytechnic University, Ben Guerir; Morocco.

³⁵CERN, Geneva; Switzerland.

³⁶Enrico Fermi Institute, University of Chicago, Chicago IL; United States of America.

³⁷LPC, Université Clermont Auvergne, CNRS/IN2P3, Clermont-Ferrand; France.

³⁸Nevis Laboratory, Columbia University, Irvington NY; United States of America.

³⁹Niels Bohr Institute, University of Copenhagen, Copenhagen; Denmark.

⁴⁰(^a)Dipartimento di Fisica, Università della Calabria, Rende; (^b)INFN Gruppo Collegato di Cosenza, Laboratori Nazionali di Frascati; Italy.

⁴¹Physics Department, Southern Methodist University, Dallas TX; United States of America.

⁴²Physics Department, University of Texas at Dallas, Richardson TX; United States of America.

⁴³National Centre for Scientific Research "Demokritos", Agia Paraskevi; Greece.

⁴⁴(^a)Department of Physics, Stockholm University; (^b)Oskar Klein Centre, Stockholm; Sweden.

⁴⁵Deutsches Elektronen-Synchrotron DESY, Hamburg and Zeuthen; Germany.

⁴⁶Lehrstuhl für Experimentelle Physik IV, Technische Universität Dortmund, Dortmund; Germany.

⁴⁷Institut für Kern- und Teilchenphysik, Technische Universität Dresden, Dresden; Germany.

⁴⁸Department of Physics, Duke University, Durham NC; United States of America.

⁴⁹SUPA - School of Physics and Astronomy, University of Edinburgh, Edinburgh; United Kingdom.

⁵⁰INFN e Laboratori Nazionali di Frascati, Frascati; Italy.

⁵¹Physikalisches Institut, Albert-Ludwigs-Universität Freiburg, Freiburg; Germany.

⁵²II. Physikalisches Institut, Georg-August-Universität Göttingen, Göttingen; Germany.

⁵³Département de Physique Nucléaire et Corpusculaire, Université de Genève, Genève; Switzerland.

⁵⁴(^a)Dipartimento di Fisica, Università di Genova, Genova; (^b)INFN Sezione di Genova; Italy.

⁵⁵II. Physikalisches Institut, Justus-Liebig-Universität Giessen, Giessen; Germany.

⁵⁶SUPA - School of Physics and Astronomy, University of Glasgow, Glasgow; United Kingdom.

⁵⁷LPSC, Université Grenoble Alpes, CNRS/IN2P3, Grenoble INP, Grenoble; France.

⁵⁸Laboratory for Particle Physics and Cosmology, Harvard University, Cambridge MA; United States of America.

⁵⁹(^a)Department of Modern Physics and State Key Laboratory of Particle Detection and Electronics, University of Science and Technology of China, Hefei; (^b)Institute of Frontier and Interdisciplinary Science and Key Laboratory of Particle Physics and Particle Irradiation (MOE), Shandong University, Qingdao; (^c)School of Physics and Astronomy, Shanghai Jiao Tong University, Key Laboratory for Particle Astrophysics and Cosmology (MOE), SKLPPC, Shanghai; (^d)Tsung-Dao Lee Institute, Shanghai; China.

⁶⁰(^a)Kirchhoff-Institut für Physik, Ruprecht-Karls-Universität Heidelberg, Heidelberg; (^b)Physikalisches Institut, Ruprecht-Karls-Universität Heidelberg, Heidelberg; Germany.

⁶¹(^a)Department of Physics, Chinese University of Hong Kong, Shatin, N.T., Hong Kong; (^b)Department of Physics, University of Hong Kong, Hong Kong; (^c)Department of Physics and Institute for Advanced Study, Hong Kong University of Science and Technology, Clear Water Bay, Kowloon, Hong Kong; China.

⁶²Department of Physics, National Tsing Hua University, Hsinchu; Taiwan.

⁶³IJCLab, Université Paris-Saclay, CNRS/IN2P3, 91405, Orsay; France.

⁶⁴Department of Physics, Indiana University, Bloomington IN; United States of America.

⁶⁵(^a)INFN Gruppo Collegato di Udine, Sezione di Trieste, Udine; (^b)ICTP, Trieste; (^c)Dipartimento Politecnico di Ingegneria e Architettura, Università di Udine, Udine; Italy.

⁶⁶(^a)INFN Sezione di Lecce; (^b)Dipartimento di Matematica e Fisica, Università del Salento, Lecce; Italy.

⁶⁷(^a)INFN Sezione di Milano; (^b)Dipartimento di Fisica, Università di Milano, Milano; Italy.

⁶⁸(^a)INFN Sezione di Napoli; (^b)Dipartimento di Fisica, Università di Napoli, Napoli; Italy.

⁶⁹(^a)INFN Sezione di Pavia; (^b)Dipartimento di Fisica, Università di Pavia, Pavia; Italy.

⁷⁰(^a)INFN Sezione di Pisa; (^b)Dipartimento di Fisica E. Fermi, Università di Pisa, Pisa; Italy.

- ⁷¹(*a*) INFN Sezione di Roma; (*b*) Dipartimento di Fisica, Sapienza Università di Roma, Roma; Italy.
- ⁷²(*a*) INFN Sezione di Roma Tor Vergata; (*b*) Dipartimento di Fisica, Università di Roma Tor Vergata, Roma; Italy.
- ⁷³(*a*) INFN Sezione di Roma Tre; (*b*) Dipartimento di Matematica e Fisica, Università Roma Tre, Roma; Italy.
- ⁷⁴(*a*) INFN-TIFPA; (*b*) Università degli Studi di Trento, Trento; Italy.
- ⁷⁵ Institut für Astro- und Teilchenphysik, Leopold-Franzens-Universität, Innsbruck; Austria.
- ⁷⁶ University of Iowa, Iowa City IA; United States of America.
- ⁷⁷ Department of Physics and Astronomy, Iowa State University, Ames IA; United States of America.
- ⁷⁸ Joint Institute for Nuclear Research, Dubna; Russia.
- ⁷⁹(*a*) Departamento de Engenharia Elétrica, Universidade Federal de Juiz de Fora (UFJF), Juiz de Fora; (*b*) Universidade Federal do Rio De Janeiro COPPE/EE/IF, Rio de Janeiro; (*c*) Instituto de Física, Universidade de São Paulo, São Paulo; (*d*) Rio de Janeiro State University, Rio de Janeiro; Brazil.
- ⁸⁰ KEK, High Energy Accelerator Research Organization, Tsukuba; Japan.
- ⁸¹ Graduate School of Science, Kobe University, Kobe; Japan.
- ⁸²(*a*) AGH University of Science and Technology, Faculty of Physics and Applied Computer Science, Krakow; (*b*) Marian Smoluchowski Institute of Physics, Jagiellonian University, Krakow; Poland.
- ⁸³ Institute of Nuclear Physics Polish Academy of Sciences, Krakow; Poland.
- ⁸⁴ Faculty of Science, Kyoto University, Kyoto; Japan.
- ⁸⁵ Kyoto University of Education, Kyoto; Japan.
- ⁸⁶ Research Center for Advanced Particle Physics and Department of Physics, Kyushu University, Fukuoka ; Japan.
- ⁸⁷ Instituto de Física La Plata, Universidad Nacional de La Plata and CONICET, La Plata; Argentina.
- ⁸⁸ Physics Department, Lancaster University, Lancaster; United Kingdom.
- ⁸⁹ Oliver Lodge Laboratory, University of Liverpool, Liverpool; United Kingdom.
- ⁹⁰ Department of Experimental Particle Physics, Jožef Stefan Institute and Department of Physics, University of Ljubljana, Ljubljana; Slovenia.
- ⁹¹ School of Physics and Astronomy, Queen Mary University of London, London; United Kingdom.
- ⁹² Department of Physics, Royal Holloway University of London, Egham; United Kingdom.
- ⁹³ Department of Physics and Astronomy, University College London, London; United Kingdom.
- ⁹⁴ Louisiana Tech University, Ruston LA; United States of America.
- ⁹⁵ Fysiska institutionen, Lunds universitet, Lund; Sweden.
- ⁹⁶ Departamento de Física Teórica C-15 and CIAFF, Universidad Autónoma de Madrid, Madrid; Spain.
- ⁹⁷ Institut für Physik, Universität Mainz, Mainz; Germany.
- ⁹⁸ School of Physics and Astronomy, University of Manchester, Manchester; United Kingdom.
- ⁹⁹ CPPM, Aix-Marseille Université, CNRS/IN2P3, Marseille; France.
- ¹⁰⁰ Department of Physics, University of Massachusetts, Amherst MA; United States of America.
- ¹⁰¹ Department of Physics, McGill University, Montreal QC; Canada.
- ¹⁰² School of Physics, University of Melbourne, Victoria; Australia.
- ¹⁰³ Department of Physics, University of Michigan, Ann Arbor MI; United States of America.
- ¹⁰⁴ Department of Physics and Astronomy, Michigan State University, East Lansing MI; United States of America.
- ¹⁰⁵ B.I. Stepanov Institute of Physics, National Academy of Sciences of Belarus, Minsk; Belarus.
- ¹⁰⁶ Research Institute for Nuclear Problems of Byelorussian State University, Minsk; Belarus.
- ¹⁰⁷ Group of Particle Physics, University of Montreal, Montreal QC; Canada.
- ¹⁰⁸ P.N. Lebedev Physical Institute of the Russian Academy of Sciences, Moscow; Russia.
- ¹⁰⁹ National Research Nuclear University MEPhI, Moscow; Russia.

- ¹¹⁰D.V. Skobel'syn Institute of Nuclear Physics, M.V. Lomonosov Moscow State University, Moscow; Russia.
- ¹¹¹Fakultät für Physik, Ludwig-Maximilians-Universität München, München; Germany.
- ¹¹²Max-Planck-Institut für Physik (Werner-Heisenberg-Institut), München; Germany.
- ¹¹³Graduate School of Science and Kobayashi-Maskawa Institute, Nagoya University, Nagoya; Japan.
- ¹¹⁴Department of Physics and Astronomy, University of New Mexico, Albuquerque NM; United States of America.
- ¹¹⁵Institute for Mathematics, Astrophysics and Particle Physics, Radboud University/Nikhef, Nijmegen; Netherlands.
- ¹¹⁶Nikhef National Institute for Subatomic Physics and University of Amsterdam, Amsterdam; Netherlands.
- ¹¹⁷Department of Physics, Northern Illinois University, DeKalb IL; United States of America.
- ¹¹⁸^(a)Budker Institute of Nuclear Physics and NSU, SB RAS, Novosibirsk; ^(b)Novosibirsk State University Novosibirsk; Russia.
- ¹¹⁹Institute for High Energy Physics of the National Research Centre Kurchatov Institute, Protvino; Russia.
- ¹²⁰Institute for Theoretical and Experimental Physics named by A.I. Alikhanov of National Research Centre "Kurchatov Institute", Moscow; Russia.
- ¹²¹^(a)New York University Abu Dhabi, Abu Dhabi; ^(b)United Arab Emirates University, Al Ain; ^(c)University of Sharjah, Sharjah; United Arab Emirates.
- ¹²²Department of Physics, New York University, New York NY; United States of America.
- ¹²³Ochanomizu University, Otsuka, Bunkyo-ku, Tokyo; Japan.
- ¹²⁴Ohio State University, Columbus OH; United States of America.
- ¹²⁵Homer L. Dodge Department of Physics and Astronomy, University of Oklahoma, Norman OK; United States of America.
- ¹²⁶Department of Physics, Oklahoma State University, Stillwater OK; United States of America.
- ¹²⁷Palacký University, Joint Laboratory of Optics, Olomouc; Czech Republic.
- ¹²⁸Institute for Fundamental Science, University of Oregon, Eugene, OR; United States of America.
- ¹²⁹Graduate School of Science, Osaka University, Osaka; Japan.
- ¹³⁰Department of Physics, University of Oslo, Oslo; Norway.
- ¹³¹Department of Physics, Oxford University, Oxford; United Kingdom.
- ¹³²LPNHE, Sorbonne Université, Université de Paris, CNRS/IN2P3, Paris; France.
- ¹³³Department of Physics, University of Pennsylvania, Philadelphia PA; United States of America.
- ¹³⁴Konstantinov Nuclear Physics Institute of National Research Centre "Kurchatov Institute", PNPI, St. Petersburg; Russia.
- ¹³⁵Department of Physics and Astronomy, University of Pittsburgh, Pittsburgh PA; United States of America.
- ¹³⁶^(a)Laboratório de Instrumentação e Física Experimental de Partículas - LIP, Lisboa; ^(b)Departamento de Física, Faculdade de Ciências, Universidade de Lisboa, Lisboa; ^(c)Departamento de Física, Universidade de Coimbra, Coimbra; ^(d)Centro de Física Nuclear da Universidade de Lisboa, Lisboa; ^(e)Departamento de Física, Universidade do Minho, Braga; ^(f)Departamento de Física Teórica y del Cosmos, Universidad de Granada, Granada (Spain); ^(g)Instituto Superior Técnico, Universidade de Lisboa, Lisboa; Portugal.
- ¹³⁷Institute of Physics of the Czech Academy of Sciences, Prague; Czech Republic.
- ¹³⁸Czech Technical University in Prague, Prague; Czech Republic.
- ¹³⁹Charles University, Faculty of Mathematics and Physics, Prague; Czech Republic.
- ¹⁴⁰Particle Physics Department, Rutherford Appleton Laboratory, Didcot; United Kingdom.
- ¹⁴¹IRFU, CEA, Université Paris-Saclay, Gif-sur-Yvette; France.
- ¹⁴²Santa Cruz Institute for Particle Physics, University of California Santa Cruz, Santa Cruz CA; United

States of America.

¹⁴³(^a)Departamento de Física, Pontificia Universidad Católica de Chile, Santiago;(^b)Millennium Institute for Subatomic physics at high energy frontier (SAPHIR), Santiago;(^c)Universidad de la Serena, La Serena;(^d)Universidad Andres Bello, Department of Physics, Santiago;(^e)Instituto de Alta Investigación, Universidad de Tarapacá, Arica;(^f)Departamento de Física, Universidad Técnica Federico Santa María, Valparaíso; Chile.

¹⁴⁴Universidade Federal de São João del Rei (UFSJ), São João del Rei; Brazil.

¹⁴⁵Department of Physics, University of Washington, Seattle WA; United States of America.

¹⁴⁶Department of Physics and Astronomy, University of Sheffield, Sheffield; United Kingdom.

¹⁴⁷Department of Physics, Shinshu University, Nagano; Japan.

¹⁴⁸Department Physik, Universität Siegen, Siegen; Germany.

¹⁴⁹Department of Physics, Simon Fraser University, Burnaby BC; Canada.

¹⁵⁰SLAC National Accelerator Laboratory, Stanford CA; United States of America.

¹⁵¹Department of Physics, Royal Institute of Technology, Stockholm; Sweden.

¹⁵²Departments of Physics and Astronomy, Stony Brook University, Stony Brook NY; United States of America.

¹⁵³Department of Physics and Astronomy, University of Sussex, Brighton; United Kingdom.

¹⁵⁴School of Physics, University of Sydney, Sydney; Australia.

¹⁵⁵Institute of Physics, Academia Sinica, Taipei; Taiwan.

¹⁵⁶(^a)E. Andronikashvili Institute of Physics, Iv. Javakhishvili Tbilisi State University, Tbilisi;(^b)High Energy Physics Institute, Tbilisi State University, Tbilisi; Georgia.

¹⁵⁷Department of Physics, Technion, Israel Institute of Technology, Haifa; Israel.

¹⁵⁸Raymond and Beverly Sackler School of Physics and Astronomy, Tel Aviv University, Tel Aviv; Israel.

¹⁵⁹Department of Physics, Aristotle University of Thessaloniki, Thessaloniki; Greece.

¹⁶⁰International Center for Elementary Particle Physics and Department of Physics, University of Tokyo, Tokyo; Japan.

¹⁶¹Department of Physics, Tokyo Institute of Technology, Tokyo; Japan.

¹⁶²Tomsk State University, Tomsk; Russia.

¹⁶³Department of Physics, University of Toronto, Toronto ON; Canada.

¹⁶⁴(^a)TRIUMF, Vancouver BC;(^b)Department of Physics and Astronomy, York University, Toronto ON; Canada.

¹⁶⁵Division of Physics and Tomonaga Center for the History of the Universe, Faculty of Pure and Applied Sciences, University of Tsukuba, Tsukuba; Japan.

¹⁶⁶Department of Physics and Astronomy, Tufts University, Medford MA; United States of America.

¹⁶⁷Department of Physics and Astronomy, University of California Irvine, Irvine CA; United States of America.

¹⁶⁸Department of Physics and Astronomy, University of Uppsala, Uppsala; Sweden.

¹⁶⁹Department of Physics, University of Illinois, Urbana IL; United States of America.

¹⁷⁰Instituto de Física Corpuscular (IFIC), Centro Mixto Universidad de Valencia - CSIC, Valencia; Spain.

¹⁷¹Department of Physics, University of British Columbia, Vancouver BC; Canada.

¹⁷²Department of Physics and Astronomy, University of Victoria, Victoria BC; Canada.

¹⁷³Fakultät für Physik und Astronomie, Julius-Maximilians-Universität Würzburg, Würzburg; Germany.

¹⁷⁴Department of Physics, University of Warwick, Coventry; United Kingdom.

¹⁷⁵Waseda University, Tokyo; Japan.

¹⁷⁶Department of Particle Physics and Astrophysics, Weizmann Institute of Science, Rehovot; Israel.

¹⁷⁷Department of Physics, University of Wisconsin, Madison WI; United States of America.

¹⁷⁸Fakultät für Mathematik und Naturwissenschaften, Fachgruppe Physik, Bergische Universität

Wuppertal, Wuppertal; Germany.

¹⁷⁹ Department of Physics, Yale University, New Haven CT; United States of America.

^a Also at Borough of Manhattan Community College, City University of New York, New York NY; United States of America.

^b Also at Bruno Kessler Foundation, Trento; Italy.

^c Also at Center for High Energy Physics, Peking University; China.

^d Also at Centro Studi e Ricerche Enrico Fermi; Italy.

^e Also at CERN, Geneva; Switzerland.

^f Also at Département de Physique Nucléaire et Corpusculaire, Université de Genève, Genève; Switzerland.

^g Also at Departament de Física de la Universitat Autònoma de Barcelona, Barcelona; Spain.

^h Also at Department of Financial and Management Engineering, University of the Aegean, Chios; Greece.

ⁱ Also at Department of Physics and Astronomy, Michigan State University, East Lansing MI; United States of America.

^j Also at Department of Physics and Astronomy, University of Louisville, Louisville, KY; United States of America.

^k Also at Department of Physics, Ben Gurion University of the Negev, Beer Sheva; Israel.

^l Also at Department of Physics, California State University, East Bay; United States of America.

^m Also at Department of Physics, California State University, Sacramento; United States of America.

ⁿ Also at Department of Physics, King's College London, London; United Kingdom.

^o Also at Department of Physics, St. Petersburg State Polytechnical University, St. Petersburg; Russia.

^p Also at Department of Physics, University of Fribourg, Fribourg; Switzerland.

^q Also at Faculty of Physics, M.V. Lomonosov Moscow State University, Moscow; Russia.

^r Also at Graduate School of Science, Osaka University, Osaka; Japan.

^s Also at Hellenic Open University, Patras; Greece.

^t Also at Institutio Catalana de Recerca i Estudis Avancats, ICREA, Barcelona; Spain.

^u Also at Institut für Experimentalphysik, Universität Hamburg, Hamburg; Germany.

^v Also at Institute of Particle Physics (IPP); Canada.

^w Also at Institute of Theoretical Physics, Iliia State University, Tbilisi; Georgia.

^x Also at Instituto de Física Teórica, IFT-UAM/CSIC, Madrid; Spain.

^y Also at Istanbul University, Dept. of Physics, Istanbul; Turkey.

^z Also at Istinye University, Istanbul; Turkey.

^{aa} Also at Joint Institute for Nuclear Research, Dubna; Russia.

^{ab} Also at Moscow Institute of Physics and Technology State University, Dolgoprudny; Russia.

^{ac} Also at National Research Nuclear University MEPhI, Moscow; Russia.

^{ad} Also at Physikalisches Institut, Albert-Ludwigs-Universität Freiburg, Freiburg; Germany.

^{ae} Also at The City College of New York, New York NY; United States of America.

^{af} Also at TRIUMF, Vancouver BC; Canada.

^{ag} Also at Università di Napoli Parthenope, Napoli; Italy.

^{ah} Also at University of Chinese Academy of Sciences (UCAS), Beijing; China.

^{ai} Also at Yeditepe University, Physics Department, Istanbul; Turkey.

* Deceased